Biomaterials 85 (2016) 111–127

Contents lists available at ScienceDirect

Biomaterials

journal homepage: www.elsevier.com/locate/biomaterials

The development of a tissue-engineered tracheobronchial epithelial model using a bilayered collagen-hyaluronate scaffold

Cian O'Leary [a, b, c, d, e, *], Brenton Cavanagh [f], Ronald E. Unger [g], C. James Kirkpatrick [g], Shirley O'Dea [h], Fergal J. O'Brien [a, c, d, e], Sally-Ann Cryan [a, b, c, d, e]

[a] Tissue Engineering Research Group, Dept. of Anatomy, Royal College of Surgeons in Ireland (RCSI), Dublin, Ireland
[b] School of Pharmacy, RCSI, Dublin, Ireland
[c] Centre for Research in Medical Devices (CURAM), RCSI, Dublin, Ireland
[d] Trinity Centre for Bioengineering, Trinity College Dublin (TCD), Dublin, Ireland
[e] Advanced Materials and Bioengineering Research (AMBER) Centre, RCSI and TCD, Dublin, Ireland
[f] Cellular and Molecular Imaging Core, RCSI, Dublin, Ireland
[g] REPAIR-Lab, Institute of Pathology, University Medical Centre, Johannes Gutenberg University, Mainz, Germany
[h] Biology Department, Maynooth University, Co Kildare, Ireland

ARTICLE INFO

Article history:
Received 21 January 2016
Received in revised form
25 January 2016
Accepted 28 January 2016
Available online 1 February 2016

Keywords:
Bilayered
Collagen
Hyaluronate
Epithelium
Co-culture
Respiratory

ABSTRACT

Today, chronic respiratory disease is one of the leading causes of mortality globally. Epithelial dysfunction can play a central role in its pathophysiology. The development of physiologically-representative *in vitro* model systems using tissue-engineered constructs might improve our understanding of epithelial tissue and disease. This study sought to engineer a bilayered collagen-hyaluronate (CHyA-B) scaffold for the development of a physiologically-representative 3D *in vitro* tracheobronchial epithelial co-culture model. CHyA-B scaffolds were fabricated by integrating a thin film top-layer into a porous sub-layer with lyophilisation. The film layer firmly connected to the sub-layer with delamination occurring at stresses of 12–15 kPa. Crosslinked scaffolds had a compressive modulus of 1.9 kPa and mean pore diameters of 70 μm and 80 μm, depending on the freezing temperature. Histological analysis showed that the Calu-3 bronchial epithelial cell line attached and grew on CHyA-B with adoption of an epithelial monolayer on the film layer. Immunofluorescence and qRT-PCR studies demonstrated that the CHyA-B scaffolds facilitated Calu-3 cell differentiation, with enhanced mucin expression, increased ciliation and the formation of intercellular tight junctions. Co-culture of Calu-3 cells with Wi38 lung fibroblasts was achieved on the scaffold to create a submucosal tissue analogue of the upper respiratory tract, validating CHyA-B as a platform to support co-culture and cellular organisation reminiscent of *in vivo* tissue architecture. In summary, this study has demonstrated that CHyA-B is a promising tool for the development of novel 3D tracheobronchial co-culture *in vitro* models with the potential to unravel new pathways in drug discovery and drug delivery.

1. Introduction

Today, chronic respiratory disease is one of the leading causes of mortality globally. Airway diseases such as chronic obstructive pulmonary disease (COPD) and cystic fibrosis (CF) have been identified as the fifth highest cause of mortality worldwide and are estimated to rise to fourth place by 2030 [1]. Additionally, tracheal, bronchial, and other lung cancers are predicted to become the sixth leading cause of mortality by the same year. At the core of many of these debilitating conditions, epithelial dysfunction can play a central role in their pathophysiology. For example, cystic fibrosis is rooted in defective ion transport across epithelia that drives bacterial colonisation and inflammation in the lungs [2]. The epithelium in the respiratory tract is of critical importance for the maintenance of homeostasis with key roles in lining the airways for protection, in mediating interaction with the external environment, and in regulating innate immune responses [3,4]. Accordingly,

* Corresponding author. School of Pharmacy, Royal College of Surgeons in Ireland (RCSI), Dublin, Ireland.
E-mail addresses: cianoleary@rcsi.ie (C. O'Leary), brentoncavanagh@rcsi.ie (B. Cavanagh), runger@uni-mainz.de (R.E. Unger), kirkpatrick@uni-mainz.de (C.J. Kirkpatrick), shirley.odea@nuim.ie (S. O'Dea), fjobrien@rcsi.ie (F.J. O'Brien), SCryan@rcsi.ie (S.-A. Cryan).

http://dx.doi.org/10.1016/j.biomaterials.2016.01.065
0142-9612/

effective drug targeting of epithelial tissue and restoration of its normal function is a significant factor in the design of therapeutics and treatment of such diseases. Furthermore, the airways are a very attractive route for systemic drug delivery to treat a range of non-respiratory diseases, with a large absorptive surface area, thin alveolar epithelium barrier, high blood flow and relatively low drug-degrading metabolic activity. Indeed, this route is of great interest for delivery of complex biotechnology medicines and advanced therapeutic medicinal products (ATMPs) [5]. With this in mind, the improvement of our understanding of epithelial tissue in healthy and diseased states can reveal novel strategies to maximise effective drug delivery and identify targets for the management or treatment of chronic disease. In order for this objective to be realised, complex, physiologically-representative *in vitro* models must be developed to address the inadequacies of current model platforms.

The use of biomimetic tissue-engineered scaffolds as a three-dimensional (3D) model is one approach by which such sophisticated models might be achieved. If designed appropriately, these constructs can incorporate an extracellular matrix analogue, pertinent cell populations and the appropriate signalling factors in the correct architectural arrangement to produce an *in vitro* system that achieves complexity and microscale structure that accurately reflects multicellular organs [6]. This is in contrast to current *in vitro* models of epithelial barriers, which typically consist of an epithelial monolayer cultured on polymeric cell inserts [7,8]. Although these models are useful for studying transepithelial transport of molecules and barrier function, they are ultimately an oversimplified model that can contribute to incomplete assessment of novel drug candidates and drug delivery technologies prior to animal testing; this increases the likeliness of failure at later stages in drug development [9]. Additionally, culture on polymeric inserts can alter cell growth and phenotype, with different proliferation, protein expression and cellular differentiation observed when different compositions of natural and synthetic substrates are utilised [10–13]. Early work by Davenport and colleagues, for example, highlighted that the presence of a type I collagen substratum induced ciliation within primary rat tracheal epithelial cells cultured at an air-liquid interface (ALI) that could not be achieved by culture on polycarbonate inserts [10]. The coating of collagen I hydrogels with type IV collagen and laminin, two basement membrane components, was found to alter basal cell attachment of oral epithelial cells and differentiation into a more mature mucosal barrier [11]. Similarly, laminin coating of poly-DL-lactic acid films enhanced expression of alveolar epithelial markers in attached embryonic stem cells [12] and influenced the barrier integrity and pigmentation in stem cell-derived retinal epithelial cells cultured on coated tissue culture plastic [13]. These examples demonstrate the applicability of natural polymers on epithelial functionality and highlight the potential of using extracellular matrix (ECM)-inspired substrates for *in vitro* culture. Furthermore, they lend credence to our hypothesis that the use of natural biomaterials homologous to the *in vivo* ECM can provide the most organotypic cell culture model and, combined with appropriate 3D tissue architecture, provide an advanced epithelial culture system.

Respiratory tissue of the tracheobronchial region in the airways is composed of a pseudostratified epithelial layer containing three main cell types-ciliated epithelial cells, goblet cells and basal cells-that are supported by a multi-cellular, fibrocartilaginous tissue basolateral to the epithelial cells [14,15]. For tracheal tissue engineering, three critical factors have been identified for successful recapitulation of the large airways: a basal lamina equivalent containing collagen fibres, mesenchymal cells such as fibroblasts, and the presence of an ALI system [16]. Indeed, a tissue-engineered approach towards *in vitro* modelling with type I collagen hydrogels has been shown to support the growth and differentiation of respiratory epithelial cells in co-culture with fibroblasts in a number of studies (reviewed in Ref. [9]). Recent interest has also arisen in the provision of naturally-derived ECM scaffolds for 3D airway modelling through the application of decellularised (DC) tissue either as DC tracheae [17], tissue slices of whole DC lung [18–21] or even the entire DC lung itself [22]. However, beyond the research of Omori and colleagues [23–25], there are few studies that use porous polymeric collagen sponges to provide a better *in vitro* representation of the fibrous tracheobronchial tissue architecture. Of course, it is desired in such porous materials that the epithelial cells do not migrate into the core of the construct and maintain their presence instead as a barrier at the scaffold surface as an interface. Thus, in this study we report on the fabrication of a bilayered collagen-based scaffold that permits the culture of bronchial epithelium on a two-dimensional (2D) film layer and the co-culture of fibroblasts in 3D in a porous layer beneath the epithelia.

The bilayered collagen scaffold proposed in this study is composed of a lyophilised collagen-hyaluronate co-polymer suspension, combining a film top-layer and porous sub-layer. Collagen membranes and hyaluronan-derivative films have shown promise for respiratory epithelial culture [16,26] but to date they have not been investigated as a co-polymer film to combine the benefits of each macromolecule alone. Regarding the sub-layer, porous collagen-hyaluronate scaffolds, previously designed by our group for cartilage regeneration, have been shown to facilitate cell growth and chondrogenic differentiation with mesenchymal stem cells [27–29]. The pore size of these scaffolds can be tailored by altering the freezing temperature of a controlled lyophilisation process which itself can influence cell adhesion, migration and growth in the construct [30–32]. These scaffolds were incorporated as the sub-layer of our epithelial *in vitro* substrate for co-culture of fibroblasts. Finally, type I collagen and hyaluronate are the predominant constituents of the tracheobronchial respiratory tract [15], and therefore the bilayered collagen-hyaluronate scaffold can further recapitulate the ECM of the tissue that is being modelled.

Thus, the major objective of this study was to engineer a bilayered collagen-hyaluronate scaffold as a tissue-engineered template for the development of a physiologically-representative 3D *in vitro* tracheobronchial epithelial co-culture model. To achieve this, this scaffold was firstly fabricated, characterised and subsequently assessed for its feasibility to support the growth and differentiation of a bronchial epithelial cell line. Finally, the scaffold was examined for its ability to support the co-culture of the epithelium with a fibroblast cell line in order to validate the scaffold as a template for 3D respiratory epithelial *in vitro* culture systems.

2. Materials and methods

2.1. Scaffold fabrication

2.1.1. CHyA film fabrication

CHyA films were fabricated using a modification of a previously described method [33]. In brief, a suspension of collagen and hyaluronate was dehydrated under airflow. The suspension of 0.5% microfibrillar bovine tendon collagen (Integra Life Sciences, Plainsboro, NJ) and 0.044% hyaluronate sodium salt derived from *Streptococcus equi* (Sigma–Aldrich, Arklow, Ireland) in 0.5 M acetic acid (Sigma) was first blended at 15,000 rpm and 4 °C for 3.5 h using an Ultra Turrax T18 Overhead blender (IKA Works Inc., Wilmington, NC) and subsequently degassed under a vacuum to remove all air bubbles created from the homogenisation process. The slurry suspension was pipetted onto a 12.5 × 12.5 cm^2

polytetrafluoroethylene plate and left overnight under an air current in a fume hood to increase dehydration of the solvent. This process produced a thin transparent CHyA copolymer film.

2.1.2. CHyA-B scaffold fabrication

A process was developed where CHyA-B scaffolds were fabricated by freeze-drying CHyA films in combination with CHyA slurry. The films were rehydrated in 0.5 M acetic acid and cut to fit onto the base of a 6×6 cm^2 stainless steel grade 304 SS pan. 4 ml or 16 ml of CHyA slurry was then pipetted over the hydrated film layer to give a scaffold thickness of 1 mm or 4 mm, respectively, and the combination was subsequently freeze-dried using either of two lyophilisation methods developed previously by our group [30,32]. In the first method, the slurry was frozen (Virtis Genesis 25EL, Biopharma, Winchester, UK) at a constant cooling rate of 1 °C/min to a final temperature of −10 °C and subsequently sublimated under a vacuum for 17 h at 0 °C [30]. The second method utilised a customised anneal cycle where the pans were initially frozen to a temperature of −20 °C before heated to −10 °C and held at this temperature for 24 h prior to sublimation [32]. For biomechanical characterisation studies, single-layer fully porous CHyA scaffolds were also fabricated using the anneal cycle (i.e. with no film layer present). After freeze-drying, the scaffolds were crosslinked and sterilised using a dehydrothermal (DHT) process at 105 °C for 24 h in a vacuum oven at 50mTorr (VacuCell 22, MMM, Germany).

2.1.3. Chemical crosslinking

DHT-crosslinked scaffolds were chemically crosslinked using 1-ethyl-3-(3-dimethylaminopropyl)carbodiimide hydrochloride (EDAC; Sigma) for certain experiments in order to increase their mechanical strength. Scaffold samples were pre-hydrated in Dulbecco's Phosphate Buffered Saline (DPBS; Sigma) and added to a solution of 6 mmol EDAC per gram of CHyA scaffold for 2 h [34]. N-hydroxysuccinimide (NHS; Sigma) was included as a catalyst at a molar ratio of EDAC: NHS 5: 2 [35]. Scaffolds were washed with DPBS to remove any residual cytotoxic product and stored in DPBS at 4 °C until use.

2.2. Scaffold characterisation

2.2.1. Scaffold ultrastructure

CHyA-B scaffolds were examined using scanning electron microscopy (SEM) in order to evaluate their architecture and to estimate film thickness. Samples were mounted to an aluminium stub using a carbon paste and sputter-coated with gold. Imaging of the scaffolds was performed using a Tescan Mira XMU scanning electron microscope. Images were captured at 5 kV using secondary electron mode, taken at a working distance between 12 and 18 mm.

2.2.2. Interfacial adhesion strength

Interfacial adhesion strength between the film and porous layers of the CHyA-B scaffolds was determined using a custom-designed interfacial strength test rig fitted to a mechanical testing machine (Z050, Zwick-Roell) as previously described [28]. 9.5 mm diameter samples were hydrated in DPBS *in situ* in the rig prior to testing to failure, which was expected to occur either at the ultimate tensile strength of one of the component layers of the scaffold or as a result of delamination at the layer interface.

2.2.3. Mechanical testing

Uni-axial, unconfined compressive testing was carried out to determine the bulk compressive elastic modulus of CHyA-B and CHyA scaffolds, a property that affects cellular growth and differentiation [34,36]. Scaffolds were cut into 9.5 mm discs with a height of 4 mm and chemically crosslinked where required as described in Section 2.1.3. DHT-crosslinked scaffolds were pre-hydrated in DPBS for 30 min prior to testing. Mechanical testing was carried out as previously described [28], with each sample tested three times. Stress was calculated from scaffold surface area and applied force, whilst strain was calculated from displacement of the scaffolds in relation to the original thickness.

2.2.4. Pore size analysis

Scaffold pore size analysis was performed to assess the effect of the film layer and lyophilisation cycle on the mean pore diameter and porosity of CHyA-B scaffold sub-layer, two important properties for cell adhesion and growth [31]. To calculate the mean pore size, scaffold samples prepared with both lyophilisation cycles were cut from random locations on the fabricated scaffold sheet and analysed using a technique described previously [32,37]. The samples were embedded in JB-4 glycolmethacrylate (Polysciences Europe, Eppelheim, Germany). Sections of 10 μm were subsequently obtained using a microtome (Leica RM 2255, Leica, Germany) and stained using toluidine blue (Sigma). Mean pore size of captured images were quantified using a pore topology analyser programme previously described [32]. For each sample, a minimum of 18 sections spanning the entire cross-section of the scaffold were analysed, resulting in the calculation of diameter of more than 1000 pores from each scaffold group.

Scaffold porosity was quantified through analysis of the relative density of the scaffold ($\rho_{scaffold}$) to its theoretical dry solid composite (ρ_{solid}; Equation (1)). The density of punched scaffold discs was calculated by measuring their mass and height using a mass balance (Mettler Toledo MX5; Mason Technology, Dublin) and digital Vernier callipers (Krunstoffwerke; Radionics, Dublin, Ireland), respectively. The solid composite scaffold density was calculated using the known density of collagen ($\rho = 1.3$ g/cm^3). The density of hyaluronate was assumed to be negligible. A minimum of 10 samples across four manufacturing batches was analysed for each group.

$$\text{Porosity}(\%) = \left(1 - \rho_{scaffold} \Big/ \rho_{solid}\right) \times 100 \quad (1)$$

2.3. Cell culture

2.3.1. Cell selection and culture media

The Calu-3 bronchial epithelium cell line (ATCC, Middlesex, UK) was used for monoculture and co-culture experiments. The cells were cultured in a 1:1 mixture of Dulbecco's modified Eagle's medium (DMEM; Sigma) and Ham's F12 medium (Sigma) supplemented with 10% foetal bovine serum (Biosera, Ringmer, UK), 2 mM L-glutamine (Sigma), 14 mM sodium bicarbonate (Sigma) and 100 U/ml penicillin/streptomycin (Sigma). This was referred to as Calu-3 medium. Cells were used between passages 20–50. The Wi38 human embryonic lung fibroblast cell line (ATCC) was used for co-culture experiments. These cells were cultured in Eagle's minimal essential medium (Sigma) supplemented with 10% foetal bovine serum, 2 mM L-glutamine, 26 mM sodium bicarbonate, 100 U/ml penicillin/streptomycin, and 1 mM sodium pyruvate (Sigma). This was referred to as Wi38 medium. Cells were used between passages 21–26 and cultured at 37 °C and 5% CO_2 in a humidified atmosphere. Unless otherwise stated, all cell culture incubation steps were also performed in these conditions.

2.3.2. Epithelial cell monoculture on CHyA-B scaffolds

CHyA-B scaffolds were assessed for their ability to support the growth and differentiation of the Calu-3 cell line under air-liquid interface (ALI) conditions. In order to facilitate ALI culture on the

scaffold, a customised cell culture system was developed using the frame of a Snapwell® cell insert (Corning Costar, NY). 15.6 mm-diameter scaffolds of 1 mm in height were pre-hydrated in DPBS and subsequently conditioned in Calu-3 medium. The polymeric membranes of the Snapwell® inserts were removed and the plastic frame was used to pin the scaffold into place and provide an effective area of 12 mm in diameter for epithelial cell seeding onto the film layer. For certain experiments, Calu-3 cells were also seeded onto pre-conditioned Transwell® inserts for comparison with scaffold culture. In both groups, cells were seeded at 5×10^5 cells/cm^2 into the apical chamber of the culture system. Three days later, media was removed from the top layer to introduce an ALI and the cells were fed via medium from the basolateral compartment for the remainder of the culture period, with media replaced every 2–3 days.

2.3.3. Co-culture in CHyA-B scaffolds

For scaffold co-culture experiments, Wi38 fibroblasts were initially seeded followed by Calu-3 cell addition. CHyA-B scaffolds were seeded using a modification of a previously described method [38]. 15.6 mm-diameter scaffolds of 1 mm in height were pre-hydrated in DPBS and conditioned with Wi38 medium. They were then seeded with 6×10^5 Wi38 cells per scaffold into the porous region of the scaffold and incubated for two hours to allow for cell attachment. The scaffolds were covered in Wi38 medium and grown for three days to allow for cell acclimatisation to the scaffold environment. Subsequently, they were then inserted into the Snapwell® system and seeded with Calu-3 cells as described above (Section 2.3.2). For cell insert co-culture, the Transwell® inserts were inverted, seeded with fibroblasts at a density of 3×10^4 cells/cm^2 and incubated for 2 h to allow for fibroblast attachment. Afterwards, the samples were returned to media-filled wells and grown for three days in Wi38 medium prior to Calu-3 seeding as outlined above (Section 2.3.2). In both groups, samples were cultured in a 1:1 mixture of Calu-3:Wi38 media following introduction of the ALI three days later with basolateral feeding for the remainder of the experiments. A summary of the ALI culture systems utilised is provided in Fig. 1.

2.4. In vitro analysis

2.4.1. Histology

Cell-seeded scaffolds were stained with haematoxylin and eosin and fast green to observe cell distribution and migration into the scaffold. Samples were fixed in 10% neutral buffered formalin (Sigma) for one hour and processed using an automated tissue processor (ASP300, Leica, Germany) overnight to dehydrate and paraffin wax-embed the samples. 10 μm sections were deparaffinised with xylene, rehydrated in descending grades of alcohol, and stained according to standard protocols. Images were captured using a microscope (Eclipse 90i, Nikon, Japan) and digital camera (DS Ri1, Nikon) with NIS Elements software (Nikon).

2.4.2. Immunofluorescence

Immunofluorescent staining was carried out to detect the presence of three markers of epithelial differentiation and functionality- MUC5AC, zonula-occludens-1 (ZO-1), and F-actin. Cell-seeded scaffolds and cell inserts were washed in DPBS and fixed in 10% neutral buffered formalin for 20 min. The samples were permeabilised with 0.1% triton x-100 (Sigma) and non-specific binding of primary antibody was inhibited by incubation with 1% bovine serum albumin (BSA; Sigma) in DPBS. They were then incubated with either 1/100 mouse anti-MUC5AC monoclonal antibody (Abcam, Cambridge, UK) or 1/100 rabbit anti-ZO-1 polyclonal antibody (Molecular Probes, Invitrogen, UK) in 1% BSA in DPBS for two hours at room temperature. A 1/500 goat anti-mouse Alexafluor®-594 or 1/500 goat anti-rabbit Alexafluor®-488 secondary antibody (Molecular Probes) in 1% BSA in DPBS was added for one hour at room temperature followed by counterstaining with Alexafluor®-488- or TRITC-labelled phalloidin (Sigma), respectively, to counterstain for F-actin. Finally, the samples were mounted in Fluoroshield® with DAPI (Sigma). Images were captured and analysed using an Axio Examiner. Z1 confocal microscope (Carl Zeiss, Cambridge, UK).

2.4.3. Scanning electron microscopy (SEM)

Cell-seeded scaffolds were imaged using SEM to assess

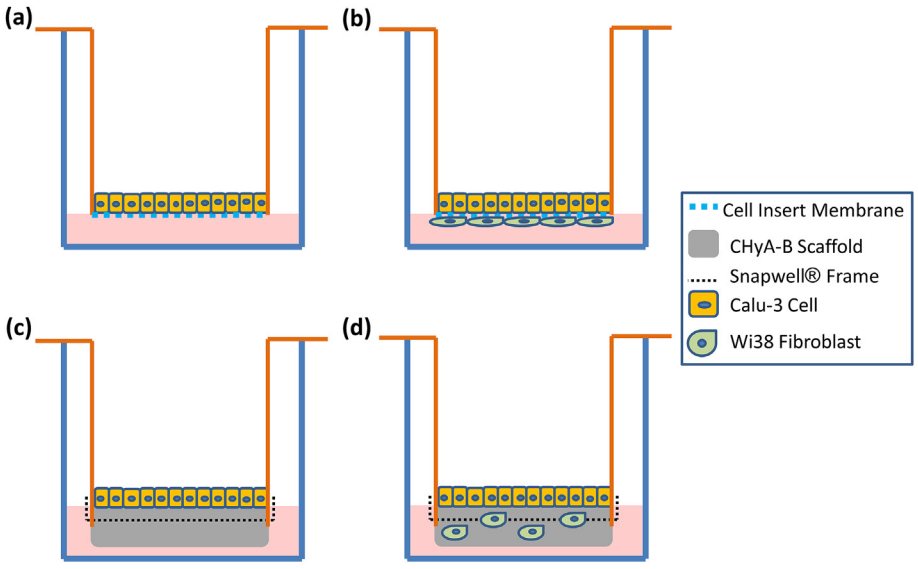

Fig. 1. Calu-3 epithelial cell and Wi38 fibroblast air-liquid interface (ALI) culture models examined for *in vitro* experiments. In all cases, Calu-3 cells are grown at the ALI. (a) Epithelial cell monoculture on a cell insert polymeric membrane. (b) Epithelial cell-fibroblast co-culture on a cell insert. Wi38 fibroblasts are seeded onto the underside of the cell insert prior to Calu-3 seeding. (c) Epithelial cell monoculture on a bilayered collagen-hyaluronate scaffold (CHyA-B). The polymeric membrane is removed from a Snapwell® cell insert and replaced with a CHyA-B scaffold held fastened using the plastic frame prior to Calu-3 seeding. (d) Epithelial cell-fibroblast co-culture on a CHyA-B scaffold. The three-dimensional porous sub-layer of the scaffolds is seeded with Wi38 fibroblasts prior to fastening the scaffold in the Snapwell® frame and Calu-3 seeding.

epithelial cell morphology and monolayer formation on the film layer of the scaffold. Samples were fixed in 3% glutaraldehyde (Sigma) for 1 h at room temperature, dehydrated in a series of ethanol and dried using supercritical carbon dioxide in a critical point dryer. They were then mounted on aluminium stubs, sputter-coated and imaged using a Tescan Mira XMU scanning electron microscope. Images were captured at 5 kV using secondary electron mode, taken at a working distance between 12 and 18 mm.

2.4.4. Transmission electron microscopy (TEM)

Cell-seeded samples were analysed by TEM to identify the presence of cilia on Calu-3 epithelial cells and to observe cell morphology. Scaffold and cell insert samples were washed in DPBS and fixed in 10% neutral buffered formalin for 20 min prior to treatment. The samples were then stained with 1% osmium tetroxide for 1 h, followed by dehydration using descending grades of methanol. They were subsequently immersed in a 1:1100% Methanol/London resin (LR) white and finally in pure LR white for one hour at room temperature. The samples were then embedded in LR white and ultrathin sections were generated using an EM UC6 ultramicrotome (Leica) and mounted on copper grids prior to examination in a Hitachi H-7650 electron microscope operating at 100 kV.

2.4.5. Quantitative reverse-transcriptase polymerase chain reaction (qRT-PCR)

Relative gene expression of Calu-3 cells seeded on scaffolds was quantified using qRT-PCR as previously described [39]. Cell-seeded scaffolds were flash frozen in liquid nitrogen and lysed in a solution containing 0.01% β-mercaptoethanol (Sigma) in RLT lysis buffer (Qiagen, Crawley, UK) for 20 min. Subsequently, they were homogenised using an Ultra Turrax T18 Overhead blender and homogeniser spin columns (Omega Biotek, Norcross, GA) to remove any residual scaffold. RNA was isolated from cell lysates using an RNeasy kit (Qiagen) and quantified using a NanoDrop 2000 spectrophotometer (Thermo Scientific, Cheshire, UK) with absorption read at 260 nm. 200 ng of total RNA was reverse transcribed to cDNA using a QuantiTect reverse transcription kit (Qiagen). RT-polymerase chain reactions were run on 7500 real-time PCR System (Applied Biosystems, UK) using a QuantiTect SYBR Green PCR Kit (Qiagen) with QuantiTect primers (Qiagen). The expression of mRNA was calculated by the delta–delta Ct ($2^{-\Delta\Delta}$CT) method relative to the housekeeping gene 18S [40]. Expression of three genetic markers was analysed: MUC5AC as a marker for mucus production, ZO-1 as a marker for tight junctions, and FOXJ1 as a marker of epithelial cell ciliation [41–43].

2.4.6. Transepithelial electrical resistance (TEER) measurement

The integrity of the epithelial barrier formed by Calu-3 cells cultured on CHyA-B scaffolds was quantified by the measurement of TEER in monoculture and co-culture systems. Prior to measurement of TEER using an EVOM voltohmmeter (World Precision Instruments, Stevenage, UK), cell culture medium was initially added to the apical compartment of the ALI cultures and samples were incubated for 1 h. Electrical resistance was measured using STX-2 chopstick electrodes (World Precision Instruments) immediately upon removal of cells from the incubator. TEER was calculated by subtracting the resistance of a cell-free scaffold or insert and correcting for the surface area available for epithelial cell growth (1.12 cm^2). To compare TEER values between groups following a plateau of the measurements [17], the average TEER values from day 11–14 were taken for each group and compared.

2.4.7. Fluorescein isothiocyante (FITC)-labelled dextran 70 (FD70) permeability assay

The integrity of the epithelial barrier formed by Calu-3 cells on CHyA-B scaffolds was further assessed through analysis of FD70 paracellular transport through the cell layer [42]. The samples were initially washed and incubated with Hank's buffered salt solution (HBSS; Sigma) in both the apical and basolateral compartments for one hour. Subsequently, the HBSS in the apical compartment was replaced with a 500 μg/ml solution of FITC-labelled dextran of an average molecular weight of 70 kDa and sampling from the basolateral compartment was performed every 30 min for two hours to quantify transported drug. An equal volume of HBSS used to replace the removed volume of basolateral solution at each time point. Additionally, a sample of the initial apical FD70 content was taken for analysis and TEER measurements were performed before and after the experiment to validate the barrier integrity was unaltered during the transport assay. The fluorescence of sampled time points was quantified by measuring excitation at 485 nm and emission at 535 nm. Fluorescence values were converted to concentration of FD70 using a standard curve and the apparent permeability coefficient (P_{app}) of FD70 was calculated using Equation (2), where F is flux (rate of change in cumulative mass transported), A is the surface area available for epithelial cell growth, and C_0 is the initial FD70 concentration in donor chamber.

$$P_{app} = F \times (1/A \cdot C_0) \quad (2)$$

2.5. Data analysis

Analysis of histological, confocal and electron microscopy images were performed using the Fiji processing software, including the measurement of length of ciliary structures. Quantitative data obtained were analysed using Microsoft Excel and GraphPad Prism 4.0 Software (GraphPad Software, San Diego, CA). In cases of analysis between two groups, statistical difference was assessed by two-tailed student t test. In cases of analysis between multiple groups, statistical difference between groups was assessed by 2-way ANOVA with Bonferroni post hoc analysis.

3. Results

3.1. Scaffold characterisation

3.1.1. Scaffold ultrastructure

CHyA-B scaffolds were examined using SEM in order to evaluate their architecture and to estimate film thickness (Fig. 2). CHyA films were successfully incorporated into a freeze-dry process to yield a bilayered porous CHyA-B scaffold. The initial dehydration process reproducibly produced a transparent co-polymer film that integrated onto the sponge-like porous layer following rehydration and lyophilisation, irrespective of the freeze-dry cycle. From analysis of the scanning electron micrographs, the film was approximately 20 μm in thickness with a smooth and uniform appearance. Below the film layer, an integrated network of pores could be seen with high interconnectivity that constituted the scaffold sub-layer.

3.1.2. Interfacial adhesion strength

The interfacial adhesion strength between the film and porous layers of the CHyA-B scaffolds was determined to quantify the degree of integration between the two layers (Fig. 3a). In all cases, strain failure occurred as a result of delamination of the film and porous layers, indicating that the strength of adhesion between layers was weaker than that of the tensile strength of the individual

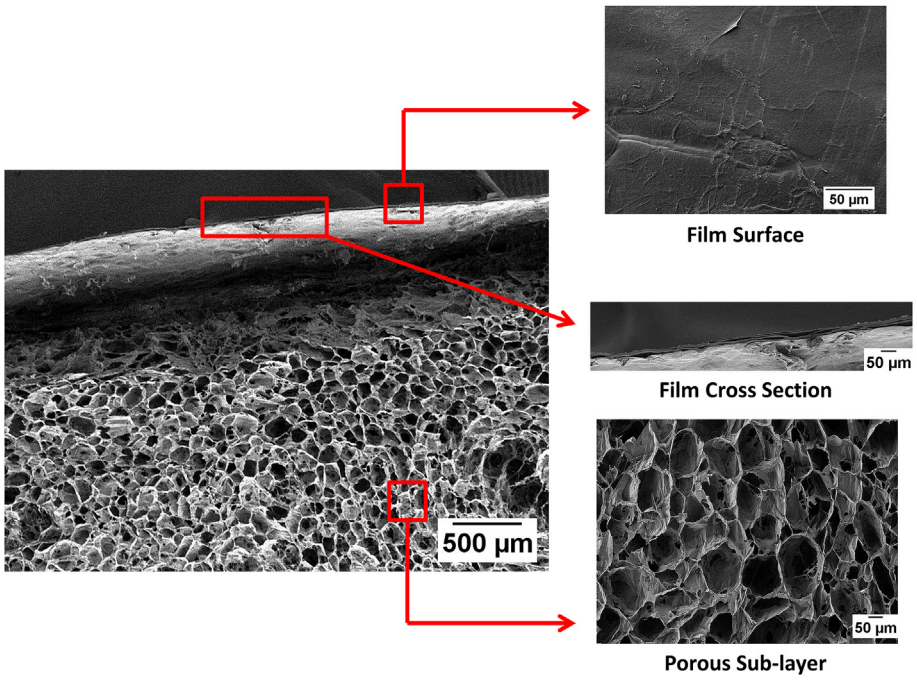

Fig. 2. Bilayered collagen-hyaluronate scaffold ultrastructure. Representative scanning electron micrograph images of a scaffold freeze-dried to a final temperature of −10 °C show the scaffold's ultrastructure, film surface and thickness, and interconnected porous sub-layer (n = 3).

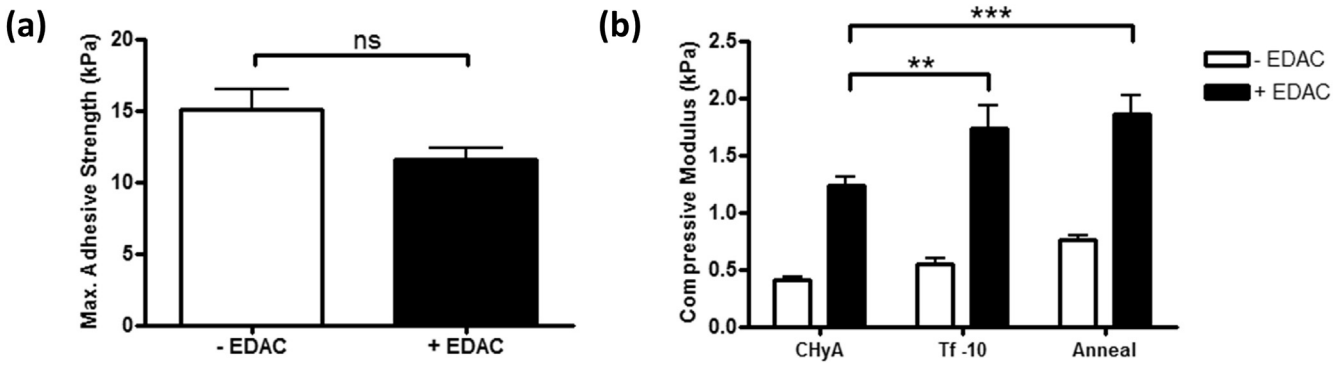

Fig. 3. Mechanical properties of bilayered collagen-hyaluronate scaffolds. (a) Layer adhesive strength of bilayered scaffolds with or without crosslinking using 1-ethyl-3-(3-dimethylaminopropyl)carbodiimide hydrochloride (EDAC; n = 4). (b) Compressive moduli of scaffolds manufactured using an anneal cycle (Anneal) or a final freezing temperature of −10 °C (Tf −10) with or without EDAC crosslinking. A single-layered fully porous collagen-hyaluronate scaffold (CHyA) is included for comparison (n = 6). Results displayed as mean ± SEM. $^{ns}p>0.05$; $^{**}p < 0.01$; $^{***}p < 0.001$.

layers. Overall, EDAC crosslinking did not significantly weaken the maximum adhesive strength of CHyA-B scaffolds prior to failure, despite observation of an apparent reduction ($p = 0.07$).

3.1.3. Mechanical testing

Uni-axial, unconfined compressive testing of CHyA-B scaffolds was carried out to determine the bulk compressive elastic modulus, a property known to affect cellular growth and differentiation [34,36] (Fig. 3b). The inclusion of the film layer into porous CHyA scaffolds was found to increase substrate stiffness, particularly in combination with EDAC crosslinking. When chemically crosslinked, CHyA-B scaffolds had a significantly larger compressive modulus, irrespective of the freeze-dry cycle. Furthermore, in the case of the scaffolds freeze-dried using an anneal step, the inclusion of the film layer in the scaffold significantly increased the compressive modulus in both the absence and presence of chemical crosslinking, changing from 0.4 kPa to 0.8 kPa in the DHT-crosslinked group ($p < 0.05$) and from 1.2 kPa to 1.9 kPa with additional EDAC crosslinking ($p < 0.001$). Overall, the chemical crosslinking with EDAC significantly increased the compressive modulus relative to DHT crosslinking alone in all groups, as expected ($p < 0.001$), and these data demonstrated that the inclusion of a film layer resulted in a stiffer scaffold.

3.1.4. Pore size analysis

Scaffold pore size analysis was performed to assess the effect of the film layer and lyophilisation cycle on the mean pore diameter and porosity of the porous sub-layer of CHyA-B scaffolds, two important properties for cell adhesion and growth [31] (Fig. 4). CHyA-B scaffolds manufactured using an anneal cycle had a mean pore size diameter of 80 μm, compared to 70 μm when lyophilised using a final freezing temperature of −10 °C (Fig. 4a; $p > 0.05$). The inclusion of a film layer did not influence the scaffold pore size, with no significant difference observed between bilayered scaffolds

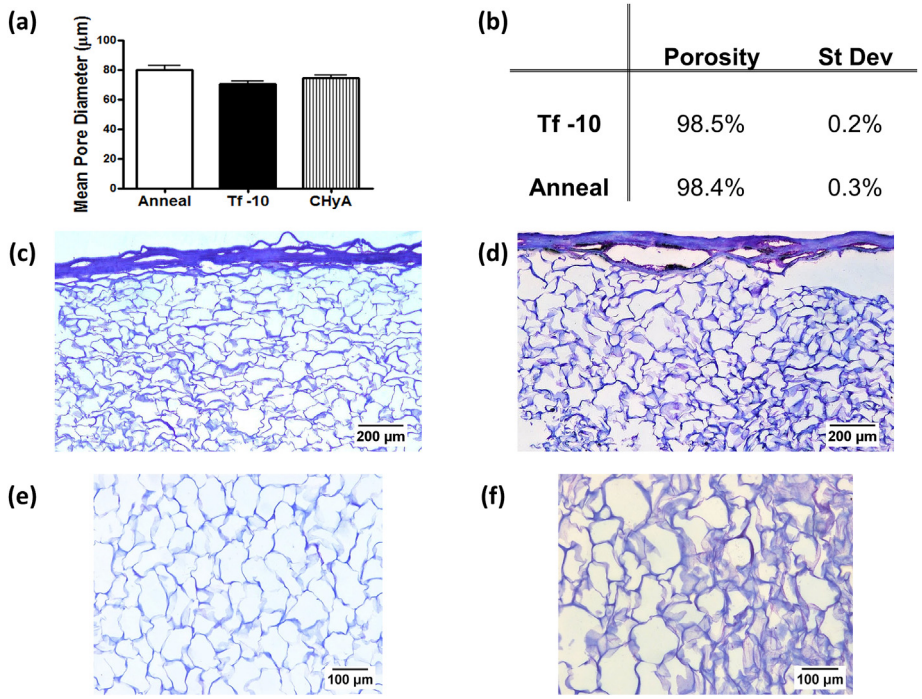

Fig. 4. Pore size analysis of bilayered collagen-hyaluronate scaffolds manufactured using an anneal cycle (Anneal) or a final freezing temperature of −10 °C (Tf −10). (a) Mean pore diameter of scaffold sub-layer (n = 3). A single-layered fully porous collagen-hyaluronate scaffold (CHyA) is included for comparison. (b) Percentage porosity of scaffold sub-layer (n = 10). (c–f) Sample toluidine blue sections of anneal (c, e) and Tf −10 scaffolds (d, f) used for software analysis. Scaffolds are visualised as a dark blue colour (n = 3). (For interpretation of the references to colour in this figure legend, the reader is referred to the web version of this article.)

and fully-porous scaffolds manufactured using the same anneal cycle. Regarding the porosity of the CHyA-B sub-layer, both fabrication processes produced highly porous materials, with a percentage porosity of greater than 98% in both scaffold groups (Fig. 4b). The anneal cycle, however, produced a porous construct that was more homogenous in its pore size distribution (Fig. 4c–f). Ultimately, the manufacture of CHyA-B with an anneal cycle resulted in a more uniformly porous scaffold with a larger pore size.

3.2. Epithelial cell culture on CHyA-B scaffolds

3.2.1. Epithelial cellular distribution and migration

Histological analysis and scanning electron microscopy were undertaken to examine Calu-3 morphology and monolayer formation on the CHyA-B apical film layer (Fig. 5). Haematoxylin and eosin and fast green images revealed that Calu-3 cells cultured on EDAC-crosslinked CHyA-B scaffolds formed an epithelial monolayer that was maintained over the culture period of 21 days (Fig. 5a). This was in contrast to cells cultured on scaffolds without EDAC crosslinking, where the samples failed to maintain their structural integrity to the extent that they had shrank and/or collapsed by day 21. Within this group, cells formed clusters of cells on the scaffold surface instead of a monolayer. On day 28, a confluent monolayer was seen on the film surface of EDAC-crosslinked CHyA-B scaffolds using SEM, confirming the histological findings (Fig. 5b). A coating of small microvilli and clusters of cilia-like structures were also observed in SEM images. Overall, these data indicated that EDAC-crosslinked CHyA-B scaffolds are suitable for Calu-3 epithelial cell monolayer culture on a 3D substrate that was still maintained after 4 weeks in culture.

3.2.2. Epithelial mucin expression in scaffold culture

The ability of the CHyA-B scaffolds to support Calu-3 cell differentiation was assessed by analysis of MUC5AC gene and glycoprotein expression (Fig. 6). Calu-3 cells cultured on scaffolds showed a significant upregulation of MUC5AC gene expression compared to that of the conventional cell insert culture control at days 7, 14, and 21 (Fig. 6a). Furthermore, MUC5AC expression was observed to increase in cells cultured on CHyA-B scaffolds over time ($p < 0.05$), unlike in cells that were cultured on the polymeric cell inserts (Fig. 6b). These data indicate that the CHyA-B scaffold promotes a sustained mucus-secreting epithelial phenotype that does not occur with conventional cell insert culture. Analysis of expressed MUC5AC glycoprotein from cells corroborated this indication (Fig. 6c–f). Immunofluorescent z-stack images detected the presence of MUC5AC on the apical side of the Calu-3 cells at day 14 (Fig. 6b, d) with greater glycoprotein fluorescence present in the scaffold cultures than in the cell insert cultures (Fig. 6e, f). Taken together, these results all indicate that the CHyA-B scaffold can influence the phenotype of the bronchial epithelial cell line at the transcriptional level and promote differentiation of the Calu-3 cells to secrete mucus.

3.2.3. Epithelial barrier formation in scaffold culture

The ability of CHyA-B scaffolds to support the differentiation of Calu-3 cells was further assessed by analysis of ZO-1 and F-actin as markers of bronchial epithelial barrier formation (Fig. 7). Calu-3 cells cultured on scaffolds exhibited a marginal upregulation of ZO-1 gene expression compared to that of the cell insert culture control at days 7 and 14, though this trend was non-significant ($p = 0.21$ and $p = 0.25$, respectively; Fig. 7a). Prolonged time in culture over 21 days also did not affect ZO-1 mRNA levels in both cell culture systems (Fig. 7b). Thus, gene expression of ZO-1 on CHyA-B scaffolds matched that of conventional cell insert ALI culture. Translation of the ZO-1 gene into protein was detected in CHyA-B scaffolds, with immunofluorescent images capturing the presence of the tight junction protein between epithelial cells at days 14 on the CHyA-B film top-layer (Fig. 7c). This indicated that

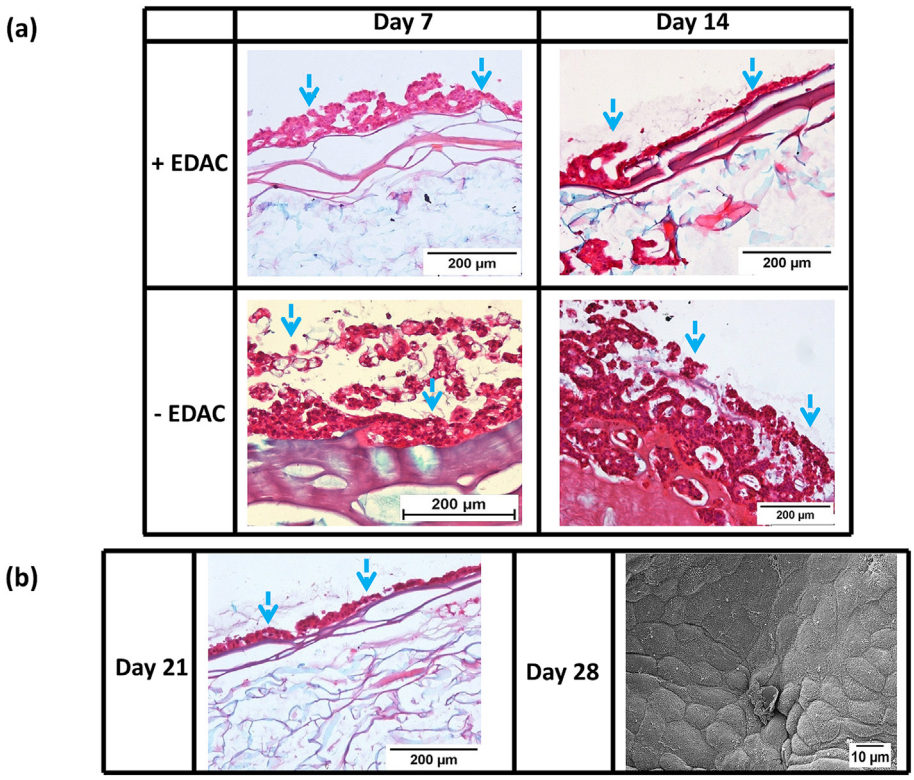

Fig. 5. (a) Calu-3 cell culture on bilayered collagen-hyaluronate scaffolds with or without crosslinking using 1-ethyl-3-(3-dimethylaminopropyl)carbodiimide hydrochloride (EDAC). (b) Long-term Calu-3 culture on EDAC-crosslinked scaffolds. Only EDAC-crosslinked scaffolds maintained cell culture beyond day 14. Haematoxylin & eosin and fast-green staining visualised scaffolds as a light-blue colour with a pink–purple film layer and cells appeared as pink–purple with darker nuclei (blue arrows; n = 9). A scanning electron micrograph at day 28 visualised a confluent monolayer with cobblestone morphology on EDAC-crosslinked scaffolds (n = 3). (For interpretation of the references to colour in this figure legend, the reader is referred to the web version of this article.)

adjacent epithelial cells formed intercellular junctions that restrict paracellular transport across the epithelium. Moreover, positive phalloidin detection highlighted the presence of F-actin bundles on the periphery of Calu-3 cells to corroborate these data (Fig. 7e); association of F-actin with ZO-1 is a noted characteristic of apical epithelial junctions [44]. As with the ZO-1 gene analysis, both culture systems displayed equivalence, with the presence and classical distribution of both junctional proteins present in all samples. Overall, these results indicate the Calu-3 cells form a functional epithelial barrier on the apical side of CHyA-B scaffolds cultured at an ALI.

3.2.4. Epithelial ciliation in scaffold culture

The third assessment of the ability of CHyA-B scaffolds to support the differentiation of Calu-3 cells examined the formation of motile cilia through analysis of the FOXJ1 gene and TEM imaging. Calu-3 cells cultured on scaffolds showed a significant upregulation of FOXJ1 compared to that of the conventional cell insert culture control at day 7 (Fig. 8a; $p < 0.01$). FOXJ1 expression in cell insert culture matched that of scaffold culture at days 14 and 21 due to a time-dependent increase in expression on cell inserts over the culture period (Fig. 8b). This indicated that the CHyA-B scaffold induced a magnitude of gene expression comparable to cell insert culture in half the amount of time. TEM analysis detected the presence of microvilli-like premature cilia on the apical side of Calu-3 cells in both samples at day 14 of culture (Fig. 8c, d); notably, the ciliary structures formed in cells cultured on CHyA-B were longer than those observed in cell insert culture (Fig. 8e, f). Additionally, TEM analysis revealed that cells grown on scaffolds adopted a pseudostratified columnar morphology along the film layer that was not observed in culture on polymeric cell inserts. Thus, these data suggest that the CHyA-B scaffold had a more rapid effect in inducing cilia formation within Calu-3 cells.

3.3. Epithelial-fibroblast co-culture on CHyA-B scaffolds

3.3.1. Cellular distribution in scaffold co-culture

Following the achievement of the formation of a confluent and differentiated Calu-3 epithelial cell barrier on EDAC-crosslinked CHyA-B scaffolds, a co-culture system of Calu-3 epithelial cells and Wi38 lung fibroblasts was examined in order to assess the scaffold's capacity to act as a substrate for three-dimensional *in vitro* co-culture models (Fig. 9). Histological staining at day 14 confirmed that in addition to the Calu-3 cell monolayer forming, Wi38 cells populated the CHyA-B porous sub-layer, with evidence of cellular migration into the scaffold towards the epithelial monolayer (Fig. 9a). Parallel monoculture of Calu-3 cells on CHyA-B scaffolds in tandem with co-cultured samples displayed an absence of any cells in the porous scaffold sub-layer but retained the epithelial cell barrier on the scaffold film layer (Fig. 9b), indicating that any cells observed in the porous layer of co-cultures were fibroblasts. Furthermore, these cells adopted a different morphology in the 3D porous structure to that observed when Calu-3 cells are cultured in such an environment (Suppl. Data 1). Overall, bilayered CHyA-B scaffolds facilitated a tracheobronchial epithelial-fibroblast co-culture with distinct cellular localisation and organisation of each cell type at the desired region on the constructs.

3.3.2. Epithelial cell differentiation in scaffold co-culture

Having developed a tracheobronchial co-culture model using

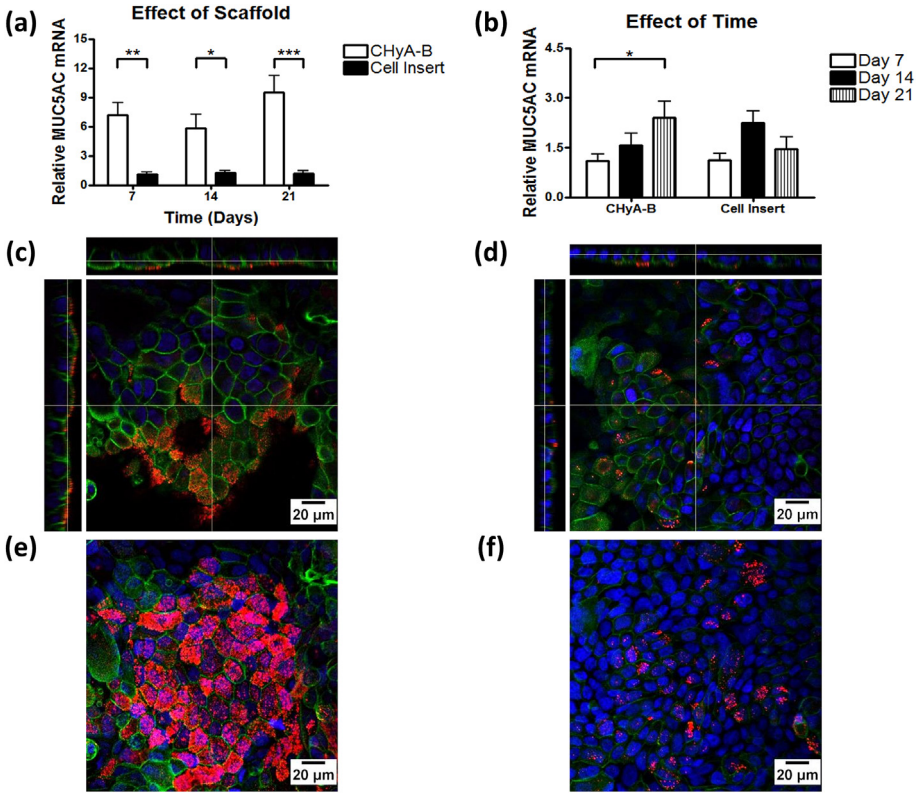

Fig. 6. Calu-3 cell mucin expression on bilayered collagen-hyaluronate (CHyA-B) scaffolds. (a, b) The effect of CHyA-B scaffolds (a) and time (b) on the relative MUC5AC mRNA expression of cells. Results are displayed as mean ± SEM with expression relative to cell insert culture at each time point (a) or to day 7 for each group (b), as appropriate (n = 7). $^{*}p < 0.05$; $^{**}p < 0.01$; $^{***}p < 0.001$. (c, d) MUC5AC glycoprotein secretion by Calu-3 cells cultured on CHyA-B scaffolds (c) and cell inserts (d) at day 14. Z-stack images display apical MUC5AC secretion (red) on top of cells counterstained for nuclei (blue) and F-actin (green; n = 6). (e, f) Maximum intensity projections of MUC5AC expression on CHyA-B scaffolds (e) and cell inserts (f) reconstructed from Z-stacks (n = 6). (For interpretation of the references to colour in this figure legend, the reader is referred to the web version of this article.)

CHyA-B scaffolds with favourable cell distribution, analysis of the three markers of Calu-3 differentiation was also performed in scaffold co-cultures to validate the maintenance, or potentially the improvement, of expression of functional biomarkers (Fig. 10). MUC5AC (Fig. 10a), ZO-1 (Fig. 10c) and cilia (Fig. 10e) were all detected in Calu-3 scaffold co-cultures as seen previously with scaffold monoculture samples. Notably, less MUC5AC was secreted from epithelial cells on CHyA-B scaffolds in co-culture than in mono-culture (Fig. 6e) but fluorescence was still greater than that observed from cell insert co-culture samples (Fig. 10b). Clear ZO-1 bands were detected in both co-culture groups (Fig. 10c, d) and longer cilia were once again observed on cells cultured on CHyA-B. Ultimately, Calu-3 and Wi38 co-culture on CHyA-B scaffolds maintained the phenotypic features of a tracheobronchial epithelium.

3.3.3. *Epithelial barrier integrity in scaffold co-culture*

In order to confirm that the differentiated epithelial layer formed upon CHyA-B scaffolds displayed an effective barrier function in both monoculture and co-culture, the integrity of the epithelial barrier was quantified by the measurement of TEER and by permeability to the large molecular weight compound FD70 (Fig. 11). In both monoculture and co-culture systems, Calu-3 cells cultured on scaffolds formed a barrier that was >500 Ωcm^2 with mean TEER values on day 14 of 681 Ωcm^2 and 691 Ωcm^2, respectively (Fig. 11a). TEER values within scaffold cultures were lower on average than those obtained from cell insert cultures. This was evident when the average TEER values of each group following day 11 were compared (Fig. 11b), where an increasing trend from CHyA-B monoculture to cell insert co-culture was recorded. In both culture systems, the inclusion of Wi38 fibroblasts increased TEER, although this trend was non-significant. Finally, the ability of the epithelial barrier to impede the paracellular transport of FD70 was observed in all samples, with low P_{app} values recorded in scaffold cultures and no transport detected in cell insert culture (Fig. 11c). These data collectively highlight the presence of a functional epithelial barrier in scaffold culture.

4. Discussion

In order to develop a more physiologically-representative alternative to current synthetic respiratory epithelial cell insert culture systems, the major objective of this study was to manufacture a tissue-engineered bilayered collagen-hyaluronate (CHyA-B) scaffold as a template for a 3D tracheobronchial *in vitro* epithelial co-culture model. Specifically, we sought to: (i) fabricate and characterise a CHyA-B scaffold, incorporating film and porous layers for epithelial and fibroblast culture, respectively; (ii) assess Calu-3 bronchial epithelial cell growth and differentiation on the film layer; and (iii) investigate whether the scaffold could support an epithelial-fibroblast co-culture model with physiologically relevant tissue architecture in order to validate the scaffold as a substrate for 3D tracheobronchial epithelial *in vitro* culture systems. The results led to the development of a novel freeze-dried CHyA-B scaffold consisting of a thin 2D film fused to a porous 3D scaffold on which Calu-3 cells were able to grow, express mucin, cilia, and form an epithelial barrier with cell retention at the ALI. Notably, EDAC crosslinking was found to be crucial for maintenance

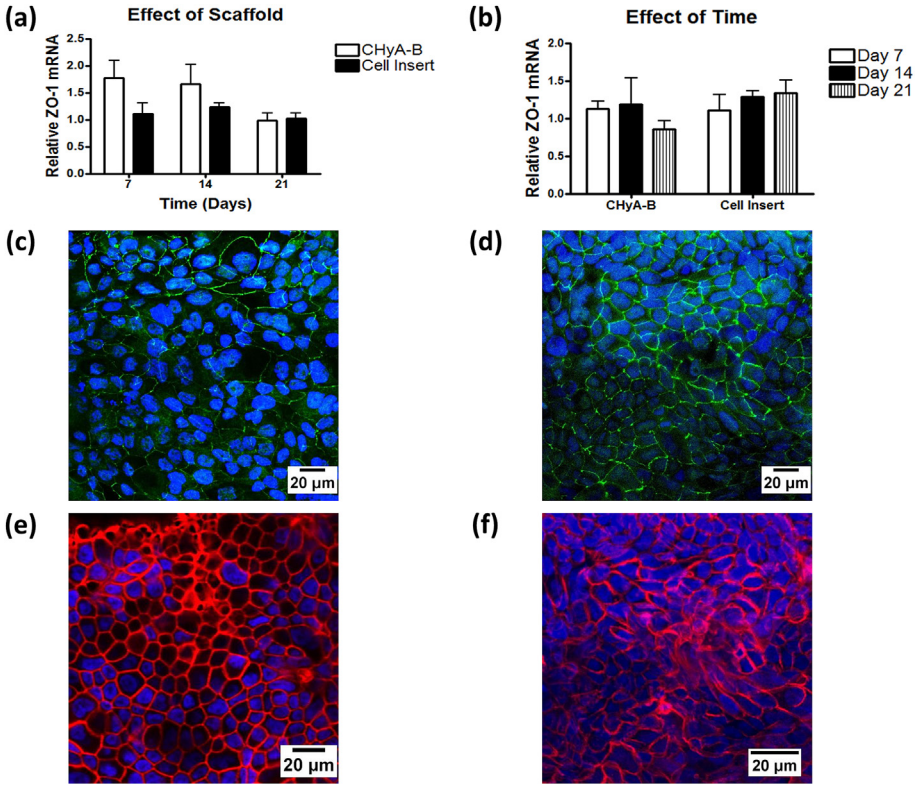

Fig. 7. Calu-3 barrier formation on bilayered collagen-hyaluronate (CHyA-B) scaffolds. (a, b) The effect of CHyA-B scaffolds (a) and time (b) on the relative ZO-1 mRNA expression of cells. Results are displayed as mean ± SEM with expression relative to cell insert culture at each time point (a) or to day 7 for each group (b), as appropriate (n = 7). (c, d) ZO-1 protein expression by Calu-3 cells cultured on CHyA-B scaffolds (c) and cell inserts (d) at day 14. Maximum intensity projections reconstructed from z-stack images display ZO-1 (green) on the borders of cells counterstained for nuclei (blue; n = 6). (e, f) F-actin expression by Calu-3 cells cultured on CHyA-B scaffolds (e) and cell inserts (f) at day 14. Maximum intensity projections reconstructed from z-stack images display F-actin (red) on the border of cells counterstained for nuclei (blue; n = 6). (For interpretation of the references to colour in this figure legend, the reader is referred to the web version of this article.)

of scaffold structure and epithelial monolayer formation. Finally, co-culture of Calu-3 cells with Wi38 lung fibroblasts was achieved on the CHyA-B scaffold, with fibroblast migration into the porous core to provide a submucosal tissue analogue of the upper respiratory tract and potential for epithelial-fibroblast crosstalk. Taken together, these data demonstrate the potential bilayered CHyA-B scaffolds as a suitable substrate for 3D *in vitro* tracheobronchial epithelial models that can be employed for drug discovery and disease-modelling purposes and advance the successful development of novel therapies for the treatment of chronic respiratory disease.

Current *in vitro* models of respiratory epithelial barriers using polymeric cell inserts are an incomplete representation of the *in vivo* tissue environment. The absence of natural ECM components and the inability to co-culture cells in a 3D physiological arrangement can contribute to an increased likelihood of failure of a potential therapeutic at later stages in drug development [9]. Alternatively, if designed appropriately and based on natural polymer materials, the use of tissue-engineered 3D models of epithelial barrier systems permits the culture of multiple cells in an environment which might be used to more accurately reflect therapeutic and toxicity responses to drugs *in vivo*. Consequently, this could improve *in vitro* screening of drug candidates and maximise the selection and translation of promising agents into effective medicines to target unmet clinical needs. Developing models of epithelial barriers in this manner is critical to achieve such a goal, both to identify new therapies for chronic diseases related to epithelial dysfunction in the airways [2] and to assess successful drug delivery across barriers following inhalable drug administration [5]. In this study, the fabricated collagen-hyaluronate scaffold was composed of a 2D film top-layer to combine the benefits of collagen- and hyaluronate-based film biomaterials in respiratory epithelial culture [16,26] with a porous 3D sub-layer which might act as a fibrocartilaginous support for mesenchymal cell culture [27–29] that contains the overall major components of the tracheobronchial ECM [15].

The CHyA-B scaffold was successfully constructed through modification of a lyophilisation technique [30,32], whereby a collagen-hyaluronate (CHyA) film was manufactured separately, rehydrated and lyophilised with CHyA suspension to create fusion of the film layer with an interconnected porous 3D sub-layer. This process was reproducible for two different freeze-dry cycles involving a final freezing temperature of −10 °C and a custom anneal cycle. The use of different freezing temperatures is known to influence the final pore size in scaffolds [30,32] and thus scaffolds were manufactured with two different freezing temperatures to verify the reproducibility of the fusion process for a range of temperatures. Successful fabrication with both cycles confirmed this reproducibility and highlighted the versatility of the manufacture process to make bilayered scaffolds using different freezing parameters. Ultrastructural analysis of the scaffold confirmed the bilayered architecture, complete with an intact film top-layer spread across a porous sublayer (Fig. 2). The two layers of the scaffold adhered to each other during lyophilisation and maintained this connection during physical manipulation and handling in experiments, although analysis of interfacial adhesion strength highlighted that this junction was the weakest structural point within the construct (Fig. 3a). Regardless, the manufacture process

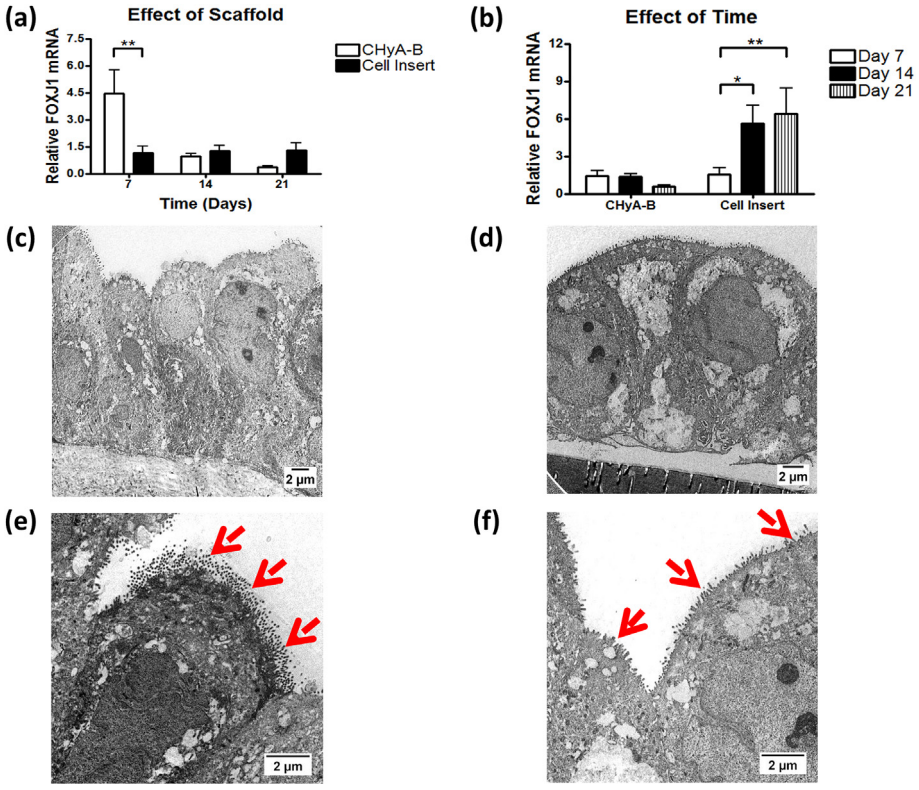

Fig. 8. Calu-3 cell ciliation on bilayered collagen-hyaluronate (CHyA-B) scaffolds. (a, b) The effect of CHyA-B scaffolds (a) and time (b) on the relative FOXJ1 mRNA expression of cells. Results are displayed as mean ± SEM with expression relative to cell insert culture at each time point (a) or to day 7 for each group (b), as appropriate (n = 7). *$p < 0.05$; **$p < 0.01$; ***$p < 0.001$. (c, d) Transmission electron micrographs of Calu-3 cells cultured on CHyA-B scaffolds (c) and cell inserts (d) at day 14. Cells cultured on scaffolds adopted a ciliated columnar morphology while cell insert culture yielded a cuboidal morphology. (e, f) Higher magnification images detected the presence of cilia on the apical side of cells in both cultures (red arrows) with longer cilia observed within cells cultured on CHyA-B scaffolds than on cell inserts. (For interpretation of the references to colour in this figure legend, the reader is referred to the web version of this article.)

successfully yielded a bilayered scaffold of adequate durability that could act as a blueprint to produce a 3D iteration of the tracheobronchial tissue structure.

Further analysis of the mechanical properties of the CHyA-B scaffold showed that the inclusion of the film layer increased substrate stiffness, particularly in combination with EDAC cross-linking (Fig. 3b). Uni-axial, unconfined compressive analysis of CHyA-B and single-layer fully porous CHyA scaffolds revealed that the presence of the film layer increased the compressive modulus from 1.2 kPa in CHyA scaffolds to 1.7–1.9 kPa in CHyA-B scaffolds, with non-significant variations seen between the methods of CHyA-B freeze-drying. Previous studies have indicated that compressive mechanical properties modulate cellular responses and lineage specification in stem cells through mechanical feedback [34,45], and research within our own group has indicated that the scaffold stiffness can influence the osteogenic and chondrogenic potential of rat MSCs cultured on CHyA scaffolds [36]. In the case of this study, however, fibroblasts were used as the secondary cell type for co-culture as opposed to a multipotent stem cell population, due to their prominent use in other respiratory models [46,47]; thus, the risk of osteogenic induction as a result of a significantly stiffer scaffold was not relevant. Indeed, given the contractile behaviour of fibroblasts in collagen-glycosaminoglycan (GAG) matrices [48], stiffer scaffolds could be of greater benefit as they are more resistant to cell-mediated contraction [49].

The third phase of CHyA-B scaffold characterisation analysed the mean pore size and porosity of the porous sub-layer (Fig. 4). Two lyophilisation cycles were performed in CHyA-B manufacture to examine the effect, if any, of the film layer on pore size and porosity. The results indicated that the sub-layer had a homogenous porous structure that was amenable as the framework for 3D co-culture with epithelia. Inclusion of the film layer gave mean pore diameters of 80 μm and 70 μm with anneal and −10 °C cycles, respectively (Fig. 4a). The inclusion of a film layer did not significantly alter the scaffold pore size, with no significant difference observed between bilayered scaffolds and fully-porous scaffolds manufactured using the same anneal cycle. Previous work carried out by our group has indicated that the optimal mean pore size of a porous biomaterial depends on a compromise between sufficiently small enough pores to increase the surface area for cell attachment [37] and sufficiently large enough pores to allow for cell migration and nutrient flow [31]. This ideal pore size can vary from one cell type to another, and the optimal pore diameter for this fibroblast cell line has not been reported to date. Therefore, the anneal cycle was selected as the fabrication method for CHyA-B co-culture studies as data with a pre-osteoblast cell line indicated that larger pores increase cell viability and migration as culture time periods progress [31]. Moreover, while both cycles produced highly porous materials (Fig. 4b), the anneal cycle gave a more homogenous distribution of pores (Fig. 4c–f), reinforcing the decision to manufacture scaffolds by this method for co-culture experiments with fibroblasts.

Following the characterisation of the CHyA-B scaffold and the identification of suitable fabrication parameters, the second objective of this study focused on the ability of the scaffold to support the growth and differentiation of the Calu-3 bronchial epithelial cell line. Histological analysis showed that EDAC cross-linking of CHyA-B scaffolds was necessary for epithelial monolayer

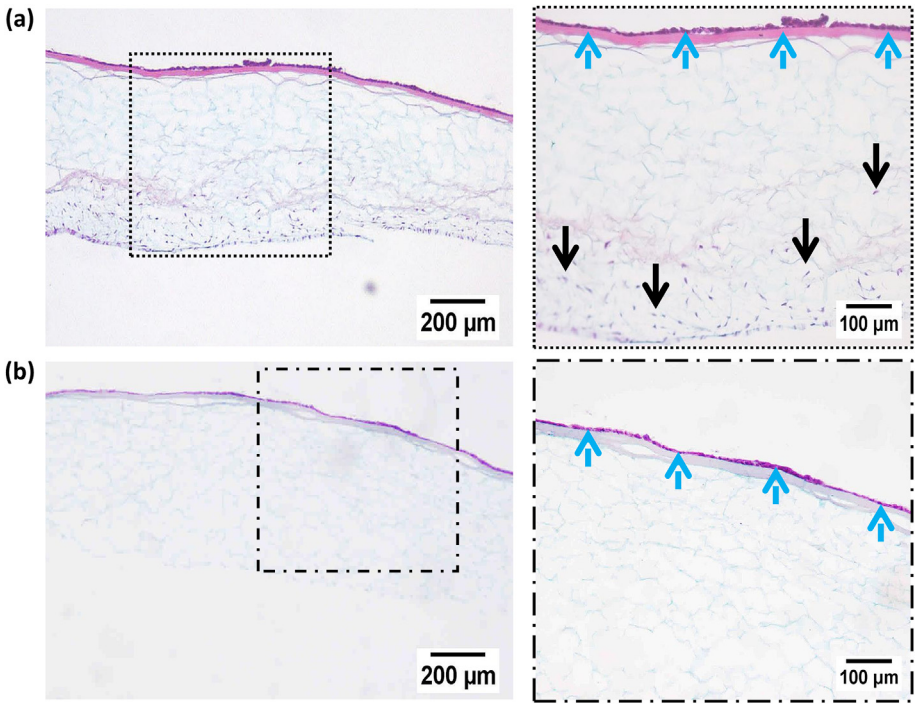

Fig. 9. Co-culture on bilayered collagen-hyaluronate scaffolds. (a) Calu-3 cells and Wi38 fibroblasts cultured together were imaged at 14 days. Higher magnification images (inset) showed Calu-3 cells forming a monolayer along the film top-layer (blue arrows) and Wi38 fibroblasts migrating into the porous sub-layer (black arrows). (b) Monoculture of Calu-3 cells on scaffolds showed the formation of a matching epithelial cell monolayer to that on co-cultured scaffolds but a notable absence of cells in the porous sub-layer. Haematoxylin & eosin and fast-green staining visualised scaffolds as a light-blue colour with a pink–purple film layer and cells appeared as pink–purple with darker nuclei (n = 9). (For interpretation of the references to colour in this figure legend, the reader is referred to the web version of this article.)

formation and cell retention at the air-liquid interface (ALI). The formation of an epithelial monolayer was only observed in the stiffer scaffolds. In the absence of EDAC crosslinking, cells tended to stay in clusters on the film layer (Fig. 5a). The Calu-3 monolayer observed at day 14 on stiffer CHyA-B scaffolds persisted through longer culture periods of 21 and 28 days (Fig. 5b), complete with a cobblestone morphology evident at the latter time point that is the hallmark of a confluent epithelial monolayer. It has been previously shown that EDAC crosslinking improves osteoblast cell numbers and distribution within collagen-GAG scaffolds [34], though at present, the cellular mechanism behind why a stiffer film facilitates epithelial monolayer formation is unknown. On the other hand, in the absence of EDAC crosslinking, the porous underside of CHyA-B samples contracted following prolonged incubation in cell culture medium, leading to gradual dissociation from the film layer and loss of biomaterial integrity by day 21. EDAC crosslinking did not increase the strength of connection between the two scaffold layers, as indicated by interfacial adhesion strength analysis (Fig. 3a); on the contrary, the stiffer scaffold appeared to exhibit lower adhesion strength prior to failure than in non-EDAC-crosslinked CHyA-B scaffolds, although this was non-significant ($p = 0.07$). Therefore, this finding suggests that the EDAC crosslinking step maintains CHyA-B scaffold integrity by reducing contraction of the porous layer, rather than by increasing the strength of interaction between scaffold layers. Taken together, these data collectively show that EDAC crosslinking is pivotal for the maintenance of the bilayered structure of CHyA-B in cell culture and contributes to epithelial monolayer formation, validating the EDAC-crosslinked CHyA-B scaffold as an effective substrate for the culture of a viable bronchial cell line as part of an *in vitro* model.

Having established EDAC-crosslinked CHyA-B scaffolds as the substrate of choice for Calu-3 epithelial culture, the study subsequently assessed Calu-3 differentiation prior to co-culture. The first differentiation marker analysed was the glycoprotein MUC5AC, a substantial component of the respiratory mucus coating and important indicator of mucociliary epithelial cell differentiation [41,50]. Culture on the CHyA-B scaffold had a direct effect in increasing and maintaining MUC5AC gene transcription at days 7, 14 and 21 relative to the standard cell insert culture (Fig. 6a). Importantly, the CHyA-B scaffold directly increased MUC5AC gene expression relative to the standard cell insert culture that is normally used to induce mucus secretion from Calu-3 cells, highlighting the effect of ECM components on epithelial cell response. This increase in expression in MUC5AC was also observed to increase over time on CHyA-B scaffolds between days 7 and 21 (Fig. 6b). The presence of hyaluronate might be responsible for these effects, as has been observed elsewhere with culture on hyaluronan-derivative films [51]. Moreover, increased expression of MUC5AC mRNA translated through to greater secretion of the glycoprotein in scaffold monoculture at day 14 than that from cell insert monoculture (Fig. 6c–f). Respiratory mucus has a prominent role in forming a defensive barrier in the respiratory tract and can hinder the delivery of aerosolised therapeutics to both the tracheobronchial epithelium itself and their transit down the airways to the alveolar region for systemic drug delivery [52]. Indeed, the effect of secreted mucins on efficacious respiratory drug delivery has become even more pertinent in chronic disorders that have a hypersecretory phenotype like asthma, bronchitis and CF [2,53,54]. In this regard, the ability of CHyA-B scaffolds to induce greater mucus secretion could therefore be of great value for drug transport assays and disease modelling. Overall, CHyA-B scaffolds were validated as a substrate to support functional mucus express from an airway epithelium.

Calu-3 cells cultured on CHyA-B scaffolds also expressed the tight junction protein ZO-1 and F-actin, indicating the formation of an epithelial barrier layer on the constructs and differentiation of

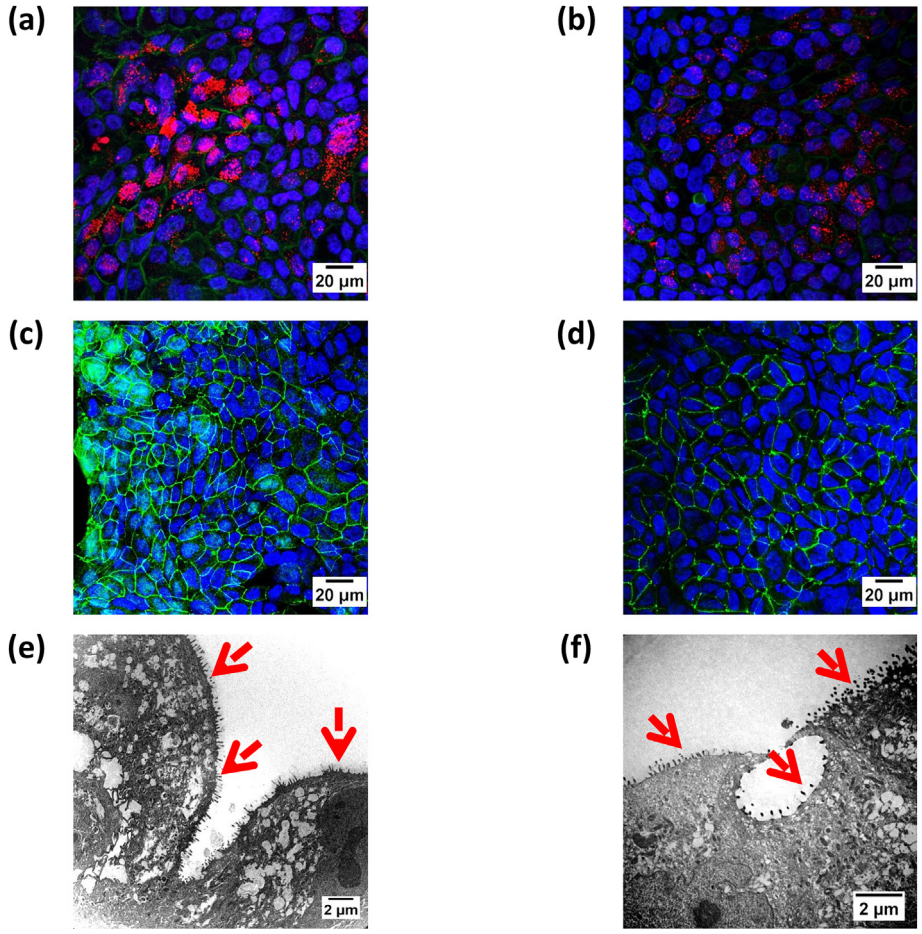

Fig. 10. Calu-3 cell differentiation in co-culture with Wi38 fibroblasts on collagen-hyaluronate (CHyA-B) scaffolds. (a, b) MUC5AC glycoprotein secretion by Calu-3 cells co-cultured on CHyA-B scaffolds (a) and cell inserts (b) at day 14. Maximum intensity projections reconstructed from Z-stacks visualise MUC5AC apical MUC5AC secretion (red) on top of cells counterstained for nuclei (blue) and F-actin (green; n = 6). (c, d) ZO-1 protein expression by Calu-3 cells co-cultured on CHyA-B scaffolds (c) and cell inserts (d) at day 14. Maximum intensity projections reconstructed from z-stack images display ZO-1 (green) on the borders of cells counterstained for nuclei (blue; n = 6). (e, f) Cilia expression by Calu-3 cells co-cultured on bilayered collagen-hyaluronate (CHyA-B) scaffolds (e) and cell inserts (f) on day 14. Transmission electron micrographs detected the presence of cilia on the apical side of cells in both cultures (red arrows) with longer cilia observed within cells cultured on CHyA-B scaffolds than on cell inserts. (For interpretation of the references to colour in this figure legend, the reader is referred to the web version of this article.)

the Calu-3 cells (Fig. 7). Scaffold culture exhibited a non-significant upregulation of ZO-1 gene expression compared to that of the conventional cell insert culture at days 7 and 14, suggesting a trend of increased expression of this barrier protein. Immunofluorescent detection of ZO-1 visualised the intercellular mesh-like network of the protein that is characteristic of its distribution in epithelial monolayers [42] (Fig. 7c). Furthermore, the detection of F-actin on the cell's circumference reinforced the hypothesis of an epithelial barrier formation (Fig. 7e); such localisation to the cell periphery and affiliation with ZO-1 is recognised as a core component of barrier integrity [44]. These data highlight the ability of the CHyA-B scaffolds to facilitate the expression of two biomarkers typical of a functional tracheobronchial epithelial barrier and contribute to its validation as a model containing an organotypic epithelium.

In addition to displaying a propensity for the induction of mucus secretion and formation of intercellular barrier junctions, the CHyA-B scaffold also had a beneficial effect on the expression of cilia in Calu-3 cells. Cilia are an integral component of the muco-ciliary escalator in the respiratory tract, extending from the apical epithelial surface to beat in a metachronal pattern and remove particulates and debris from the airways [55], and are thus an important feature of a fully-functional tracheobronchial epithelium. Analysis of expression of FOXJ1, a master regulator of motile cilogenesis [43,55], revealed that CHyA-B scaffolds upregulated this gene by an order of magnitude similar to that in Calu-3 cells on cell inserts, but in half the amount of time (Fig. 8a, b). Cilogenesis is one feature of respiratory epithelial cell culture that typically takes between 21 and 28 days [46] and so the finding of an early upregulation of FOXJ1 is noteworthy and suggests an earlier promotion of cilogenesis in bronchial epithelial cells cultured on CHyA-B scaffolds and therefore, more rapid development of an *in vitro* model for subsequent toxicity testing or disease studies. In the case of Calu-3 cells, the ciliaton was assessed after 14 days in culture in line with the literature [42] and at this time point, the microvilli structures observed in scaffold monoculture were longer than those in cell insert monoculture (1 μm vs 0.5 μm) and thinner in shape (Fig. 8e, f). Neither culture system produced fully-elongated cilia; this might be due in part to the inherent limited ciliary potential of the Calu-3 cell line. Discrepancies between primary tracheobronchial and Calu-3 transcriptional profiles have been reported [56] which could culminate in the absence of other co-factors needed for complete ciliation. Nevertheless, in this study, the improved effect inductive effect provided by CHyA-B scaffolds in comparison to cell insert culture was demonstrated.

This study sought to not only investigate whether the scaffold could support a bronchial epithelial cell line in monoculture, but

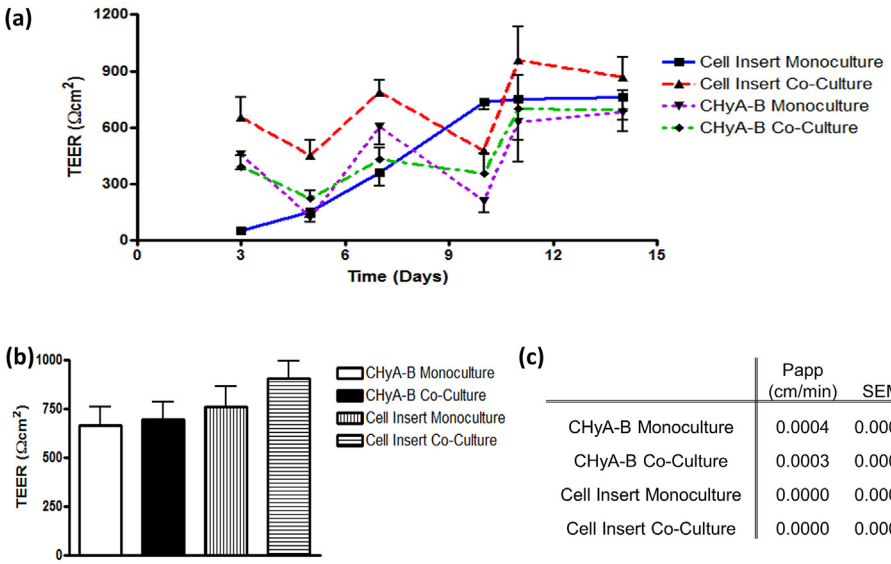

(c)

	Papp (cm/min)	SEM
CHyA-B Monoculture	0.0004	0.0001
CHyA-B Co-Culture	0.0003	0.0001
Cell Insert Monoculture	0.0000	0.0000
Cell Insert Co-Culture	0.0000	0.0000

Fig. 11. Calu-3 epithelial cell barrier integrity in monoculture and co-culture on bilayered collagen-hyaluronate (CHyA-B) scaffolds. Calu-3 cells were either cultured in monoculture or in co-culture with Wi38 fibroblasts for 14 days at an air-liquid interface. Cells were also cultured on cell inserts in monoculture and in co-culture. (a) Transepithelial electrical resistance (TEER) of Calu-3 cells. Results displayed as mean ± SEM (n = 15). (b) Average TEER values of Calu-3 epithelial cell barriers following plateau of electrical resistance (>day 10). Results displayed as mean ± SEM (n = 22). (c) Apparent permeability coefficient (Papp) of fluorescein isothiocyanate-labelled dextran 70 (FITC-dextran) through the Calu-3 cell barrier at Day 14 (n = 9).

also to develop an epithelial-fibroblast co-culture model with improved physiological tissue architecture in order to validate the scaffold as a substrate for 3D airway epithelial *in vitro* culture. To this end, Calu-3 cells were cultured together with Wi38 fibroblasts on CHyA-B scaffolds in order to establish whether the fibroblasts could migrate into the porous scaffold towards the epithelial monolayer. Histological analysis provided evidence of Wi38 attachment and cellular migration into the scaffold towards the epithelial monolayer (Fig. 9). While the native ECM of the trachea and bronchi is more densely packed than the submucosal framework present in CHyA-B in its cell-free form, the construct developed provides an improved 3D representation of the native ECM for 3D co-culture than the flat 2D nature of cell inserts and holds greater potential for recapitulation of the native tissue. Collagen-glycosaminoglycan scaffolds have consistently demonstrated their ability to support the attachment, proliferation and functionalisation of such cells in a 3D environment [27,28,31,36,48] and exhibit the suitable porosity to allow for cellular migration into the scaffold and nutrient flow [31]. Moreover, the porous nature can provide suitable void space for fibroblasts to fill with their own deposited ECM matrix following anchorage to the scaffold struts [57]. Thus, the CHyA-B scaffold's architecture can potentially facilitate epithelial-fibroblast crosstalk in addition to mimicking the *in vivo* tracheobronchial arrangement of mesenchymal cells embedded in the ECM beneath the epithelial monolayer.

The analysis of indicators of differentiation within the CHyA-B co-culture system demonstrated that the three principal hallmarks of a functional tracheobronchial barrier-mucus secretion, barrier formation and ciliation-continued to be expressed by Calu-3 cells, and that the presence of fibroblasts altered the pattern of epithelial mucus secretion on the scaffolds (Fig. 10). Of particular note, MUC5AC expression was lower than that observed in scaffold monoculture (Fig. 6e), although still greater in intensity than that observed in cell insert mono-culture and co-culture. This result indicates that both the scaffold biomaterial and the Wi38 fibroblasts modulate epithelial mucin expression in the CHyA-B co-culture system, with the resultant MUC5AC levels representing a culmination of signalling events regulated by material and cell factors. The addition of fibroblasts to cell insert culture did not alter MUC5AC expression by Calu-3 cells. A recent study by Harrington at al. reported that the inclusion of lung fibroblasts to Calu-3 culture on an electrospun polyethylene terephthalate scaffold (PET) scaffold induced apical MUC5AC expression [58]. Interestingly, no MUC5AC secretion was detected in Calu-3 monoculture on electrospun PET which contrasts with the data presented here of PET cell inserts that detected MUC5AC in mono- and co-culture (Fig. 6f). We postulate that this difference is a result of the substrate topography of the electrospun material. Nevertheless, our CHyA-B data shows that both our natural polymeric scaffold and fibroblast factors are influencing mucus secretion in our model.

Immunofluorescent staining of ZO-1 did not discern any difference in ZO-1 staining in CHyA-B mono- and co-culture systems. This was reflected in the quantitative barrier analysis using transepithelial electrical resistance (TEER; Fig. 11a, b). Scaffold TEER values were lower than those obtained for cell insert cultures, albeit non-significantly. Co-culture increased the TEER with scaffolds and cell inserts relative to monoculture, as has been regularly observed in the literature [17,46,58]. Data on TEER values from *ex vivo* human lung tissue have not been reported to date but analysis of rabbit tissue and human primary epithelial cell cultures indicate a range of 300–650 Ωcm^2 [59]. Thus, the lower TEER values obtained from cell barriers following plateau on CHyA-B in mono-culture and co-culture (662 Ωcm^2 and 694 Ωcm^2, respectively) offer a closer physiological reflection than that with cell insert mono- and co-culture (756 Ωcm^2 and 902 Ωcm^2, respectively). In all cases, analysis of paracellular permeability using FD70 confirmed that all epithelial barriers formed were suitably robust (Fig. 11c) and further justified the hypothesis that CHyA-B scaffolds displayed a positive effect on the organotypic culture of a physiologically relevant *in vitro* tracheobronchial epithelium.

Current co-culture models of the respiratory tract primarily consist of cell culture on the apical and basolateral sides of polymeric cell inserts [46,60] or using collagen hydrogels [9,47,61]. We propose that our CHyA-B scaffold confers several advantages over these approaches. Firstly, the use of a porous CHyA sub-layer includes an ECM component absent in polymeric inserts. Secondly,

the porous layer provides a framework for fibroblast culture in 3D instead of on a flat 2D insert, which can influence cell behaviour through biomechanical signalling pathways and cytoskeletal rearrangement [62]. While this is an advantage that a collagen hydrogel embedded with fibroblasts can also offer, porous, sponge-like constructs like CHyA-B provide increased stability, mechanical strength and practicality. These freeze-dried constructs can be manufactured and crosslinked without the need for *in situ* gelation, ultimately resulting in more convenient and reproducible 3D culture. Moreover, CHyA-B further improves upon the *in vitro* representation of the fibrous tissue architecture and composition of the conducting region of the respiratory tract relative to type I collagen hydrogels [15].

Recent studies have examined the use of decellularised (DC) lung tissue for applications in 3D *in vitro* modelling of the airways as an alternative, either as DC tracheae [17], tissue slices of whole DC lung [18–21] or even the entire DC lung itself [22]. The use of DC tissue has the major advantage of preserving the tissue architecture of the organ of interest in addition to the majority of native ECM components [63], Interestingly, a recent study has used solubilised DC tissue as a source of native ECM that can be reconstructed into a porous scaffold material for modelling tissue in a specialised scaffold construct using an innovative process that extrudes the ECM as a bioink using a 3D printer [64]. This bioink can also be loaded with cells prior to 3D printing and has been tested with adipose, cartilage and heart tissues; future studies with respiratory tissue may yield a novel biomaterial scaffold derived from ECM components that can further recapitulate organ-specific cell-signalling mechanisms. Decellularisation processes, however can remove glycosaminoglycans such as hyaluronate and weaken mechanical properties [65]. Issues also remain with the ideal method of decellularisation for lung tissue and storage conditions [66,67]. Of course, DC tissue ultimately requires donor tissue which can lead to problems with supply issues. Therefore, with consideration to cell insert co-cultures, collagen hydrogels, and DC lung tissue, the tissue-engineered bilayered CHyA-B scaffold presented in this study is a suitable compromise as a 3D tracheobronchial *in vitro* epithelial co-culture model that provides co-culture in 3D, relevant composition, suitable handling properties and reproducibility in manufacture, storage, and a ready supply of raw material.

Of course, while this study has successfully achieved its objectives and developed a novel scaffold and co-culture system for 3D *in vitro* modelling of the upper respiratory tract, it suffers from one principal limitation-the use of a bronchial epithelial cell line instead of primary human tracheobronchial epithelial cells. It is well-known that current bronchial cell lines do not exhibit the exact phenotypic traits to that of pseudostratified columnar epithelium *in vivo* [59]; indeed, the limited ciliation potential of Calu-3 cells has been highlighted in this study, for example. Differences have also been noted between cell line and primary cell cultures in toxicological response to known carcinogens [68]. Accordingly, it is our long-term objective to develop a primary tracheobronchial cell co-culture system with the CHyA-B scaffold to further recapitulate the *in vivo* anatomy and physiology in this 3D model. Nevertheless, it is advantageous to use a standardised cell line for the development of a novel tissue-engineered scaffold design with a new application as the risk of confounding results related to donor variability are avoided at the early stages of development; this recommendation is in line with guidance for the development of novel assays with respiratory cells [69]. Moreover, respiratory cell lines such as Calu-3 cells remain of great interest for respiratory drug development [59,70] and have previously been investigated for other synthetic constructs [58]. It is therefore of interest as the choice of epithelial cell in its own right and this study has added to our understanding of the positive influence of a naturally-derived polymeric scaffold on the differentiation of the Calu-3 cell line towards a more pseudostratified tracheobronchial epithelium with the hallmark functional features.

5. Conclusions

In summary, this study has developed a bilayered collagen-hyaluronate scaffold as a 3D *in vitro* model of the tracheobronchial region of the respiratory tract. This scaffold combines a film layer for the epithelial cell culture and a porous 3D sub-layer for co-culture with other cell types. The construct demonstrated the ability to support the growth and differentiation of a respiratory cell line in addition to epithelial-fibroblast co-culture. This biomaterial can act as a customisable platform technology to generate a physiologically-representative 3D system to advance our understanding of airway epithelial regulation, dysregulation in disease, and subsequent drug discovery and delivery for effective treatment. Overall, CHyA-B scaffolds are a promising tool that can open new avenues towards the treatment of chronic respiratory disease.

Author disclosure

No competing financial interests exist.

Acknowledgements

The authors acknowledge the funding received for this research under the Programme for Research in Third Level Institutions Cycle 5 & co-funded through the European Regional Development Fund, part of the European Union Structural Funds Programme 2007–2013, and the support of the European Molecular Biology Organisation (EMBO) short-term fellowship (ASTF 567-2014). This publication has also been supported in part by a research grant from Science Foundation Ireland (SFI) under Grant Number SFI/12/RC/2278, in addition to funding from the European Research Council (grant agreement no. 239685) under the EU Seventh Framework Programme (FP7/2007–2013). SAC is a SFI investigator (13/1A/1840). Collagen was kindly provided by Integra Life Sciences Corporation. COL would like to thank Alan J. Ryan, Royal College of Surgeons in Ireland, for helpful advice on the methods of pore size analysis.

Appendix A. Supplementary data

Supplementary data related to this article can be found at http://dx.doi.org/10.1016/j.biomaterials.2016.01.065.

References

[1] C.D. Mathers, D. Loncar, Projections of global mortality and burden of disease from 2002 to 2030, PLoS Med. 3 (2006) e442.
[2] D. Hartl, A. Gaggar, E. Bruscia, A. Hector, V. Marcos, A. Jung, et al., Innate immunity in cystic fibrosis lung disease, J. Cyst. Fibros. 11 (2012) 363–382.
[3] D.A. Knight, S.T. Holgate, The airway epithelium: structural and functional properties in health and disease, Respirology 8 (2003) 432–446.
[4] A. Tam, S. Wadsworth, D. Dorscheid, S.F. Man, D.D. Sin, The airway epithelium: more than just a structural barrier, Ther. Adv. Respir. Dis. 5 (2011) 255–273.
[5] S.A. Shoyele, A. Slowey, Prospects of formulating proteins/peptides as aerosols for pulmonary drug delivery, Int. J. Pharm. 314 (2006) 1–8.
[6] N.E. Vrana, P. Lavalle, M.R. Dokmeci, F. Dehghani, A.M. Ghaemmaghami, A. Khademhosseini, Engineering functional epithelium for regenerative medicine and in vitro organ models: a review, Tissue Eng. Part B Rev. 19 (2013) 529–543.
[7] S.G. Klein, J. Hennen, T. Serchi, B. Blomeke, A.C. Gutleb, Potential of coculture in vitro models to study inflammatory and sensitizing effects of particles on the lung, Toxicol. In Vitro 25 (2011) 1516–1534.
[8] N. Navabi, M.A. McGuckin, S.K. Linden, Gastrointestinal cell lines form polarized epithelia with an adherent mucus layer when cultured in semi-wet

interfaces with mechanical stimulation, PLoS One 8 (2013) e68761.
[9] C. O'Leary, J.L. Gilbert, S. O'Dea, F.J. O'Brien, S.A. Cryan, Respiratory tissue engineering: current status and opportunities for the future, Tissue Eng. Part B Rev. 21 (2015) 323–344.
[10] E.A. Davenport, P. Nettesheim, Regulation of mucociliary differentiation of rat tracheal epithelial cells by type I collagen gel substratum, Am. J. Respir. Cell Mol. Biol. 14 (1996) 19–26.
[11] S.W. Kim, K.C. Park, H.J. Kim, K.H. Cho, J.H. Chung, K.H. Kim, et al., Effects of collagen IV and laminin on the reconstruction of human oral mucosa, J. Biomed. Mater. Res. 58 (2001) 108–112.
[12] Y.M. Lin, A. Zhang, H.J. Rippon, A. Bismarck, A.E. Bishop, Tissue engineering of lung: the effect of extracellular matrix on the differentiation of embryonic stem cells to pneumocytes, Tissue Eng. Part A 16 (2010) 1515–1526.
[13] A. Sorkio, H. Hongisto, K. Kaarniranta, H. Uusitalo, K. Juuti-Uusitalo, H. Skottman, Structure and barrier properties of human embryonic stem cell-derived retinal pigment epithelial cells are affected by extracellular matrix protein coating, Tissue Eng. Part A 20 (2014) 622–634.
[14] S. Huang, L. Wiszniewski, S. Constant, The use of *in vitro* 3D cell models in drug development for respiratory diseases, in: I.M. Kapetanovic (Ed.), Drug Discovery and Development – Present and Future, InTech, Croatia, 2011, pp. 169–190.
[15] S.E. Dunsmore, D.E. Rannels, Extracellular matrix biology in the lung, Am. J. Physiol. 270 (1996) L3–L27.
[16] C. Pfenninger, I. Leinhase, M. Endres, N. Rotter, A. Loch, J. Ringe, et al., Tracheal remodeling: comparison of different composite cultures consisting of human respiratory epithelial cells and human chondrocytes, In Vitro Cell. Develop. Biol. Anim. 43 (2007) 28–36.
[17] E. Melo, J.Y. Kasper, R.E. Unger, R. Farre, C.J. Kirkpatrick, Development of a bronchial wall model: triple culture on a decellularized porcine trachea, Tissue Eng. Part C Methods 21 (2015) 909–921.
[18] A.J. Booth, R. Hadley, A.M. Cornett, A.A. Dreffs, S.A. Matthes, J.L. Tsui, et al., Acellular normal and fibrotic human lung matrices as a culture system for in vitro investigation, Am. J. Respir. Crit. Care Med. 186 (2012) 866–876.
[19] H. Sun, E. Calle, X. Chen, A. Mathur, Y. Zhu, J. Mendez, et al., Fibroblast engraftment in the decellularized mouse lung occurs via a beta1-integrin-dependent, FAK-dependent pathway that is mediated by ERK and opposed by AKT, Am. J. Physiol. Lung Cell. Mol. Physiol. 306 (2014) L463–L475.
[20] D.E. Wagner, N.R. Bonenfant, D. Sokocevic, M.J. Desarno, Z.D. Borg, C.S. Parsons, et al., Three-dimensional scaffolds of acellular human and porcine lungs for high throughput studies of lung disease and regeneration, Biomaterials 35 (2014) 2664–2679.
[21] D.E. Wagner, S.L. Fenn, N.R. Bonenfant, E.R. Marks, Z.D. Borg, P. Saunders, et al., Design and synthesis of an artificial pulmonary pleura for high throughput studies in acellular human lungs, Cell. Mol. Bioeng. 7 (2014) 184–195.
[22] D.K. Mishra, M.J. Thrall, B.N. Baird, H.C. Ott, S.H. Blackmon, J.M. Kurie, et al., Human lung cancer cells grown on acellular rat lung matrix create perfusable tumor nodules, Ann. Thorac. Surg. 93 (2012) 1075–1081.
[23] Y. Nomoto, K. Kobayashi, Y. Tada, I. Wada, T. Nakamura, K. Omori, Effect of fibroblasts on epithelial regeneration on the surface of a bioengineered trachea, Ann. Otol. Rhinol. Laryngol. 117 (2008) 59–64.
[24] K. Kobayashi, T. Suzuki, Y. Nomoto, Y. Tada, M. Miyake, A. Hazama, et al., A tissue-engineered trachea derived from a framed collagen scaffold, gingival fibroblasts and adipose-derived stem cells, Biomaterials 31 (2010) 4855–4863.
[25] A. Tani, Y. Tada, T. Takezawa, M. Imaizumi, Y. Nomoto, T. Nakamura, et al., Regeneration of tracheal epithelium using a collagen vitrigel-sponge scaffold containing basic fibroblast growth factor, Ann. Otol. Rhinol. Laryngol. 121 (2012) 261–268.
[26] T.W. Huang, Y.H. Chan, P.W. Cheng, Y.H. Young, P.J. Lou, T.H. Young, Increased mucociliary differentiation of human respiratory epithelial cells on hyaluronan-derivative membranes, Acta Biomater. 6 (2010) 1191–1199.
[27] A. Matsiko, T.J. Levingstone, F.J. O'Brien, J.P. Gleeson, Addition of hyaluronic acid improves cellular infiltration and promotes early-stage chondrogenesis in a collagen-based scaffold for cartilage tissue engineering, J. Mech. Behav. Biomed. Mater. 11 (2012) 41–52.
[28] T.J. Levingstone, A. Matsiko, G.R. Dickson, F.J. O'Brien, J.P. Gleeson, A biomimetic multi-layered collagen-based scaffold for osteochondral repair, Acta Biomater. 10 (2014) 1996–2004.
[29] A. Matsiko, J.P. Gleeson, F.J. O'Brien, Scaffold mean pore size influences mesenchymal stem cell chondrogenic differentiation and matrix deposition, Tissue Eng. Part A 21 (2015) 486–497.
[30] F.J. O'Brien, B.A. Harley, I.V. Yannas, L. Gibson, Influence of freezing rate on pore structure in freeze-dried collagen-GAG scaffolds, Biomaterials 25 (2004) 1077–1086.
[31] C.M. Murphy, M.G. Haugh, F.J. O'Brien, The effect of mean pore size on cell attachment, proliferation and migration in collagen-glycosaminoglycan scaffolds for bone tissue engineering, Biomaterials 31 (2010) 461–466.
[32] M.G. Haugh, C.M. Murphy, F.J. O'Brien, Novel freeze-drying methods to produce a range of collagen-glycosaminoglycan scaffolds with tailored mean pore sizes, Tissue Eng. Part C Methods 16 (2010) 887–894.
[33] S.R. Caliari, M.A. Ramirez, B.A. Harley, The development of collagen-GAG scaffold-membrane composites for tendon tissue engineering, Biomaterials 32 (2011) 8990–8998.
[34] M.G. Haugh, C.M. Murphy, R.C. McKiernan, C. Altenbuchner, F.J. O'Brien, Crosslinking and mechanical properties significantly influence cell attachment, proliferation, and migration within collagen glycosaminoglycan scaffolds, Tissue Eng. Part A 17 (2011) 1201–1208.
[35] L.H. Olde Damink, P.J. Dijkstra, M.J. van Luyn, P.B. van Wachem, P. Nieuwenhuis, J. Feijen, Cross-linking of dermal sheep collagen using a water-soluble carbodiimide, Biomaterials 17 (1996) 765–773.
[36] C.M. Murphy, A. Matsiko, M.G. Haugh, J.P. Gleeson, F.J. O'Brien, Mesenchymal stem cell fate is regulated by the composition and mechanical properties of collagen-glycosaminoglycan scaffolds, J. Mech. Behav. Biomed. Mater. 11 (2012) 53–62.
[37] F.J. O'Brien, B.A. Harley, I.V. Yannas, L.J. Gibson, The effect of pore size on cell adhesion in collagen-GAG scaffolds, Biomaterials 26 (2005) 433–441.
[38] J.C. Bridge, J.W. Aylott, C.E. Brightling, A.M. Ghaemmaghami, A.J. Knox, M.P. Lewis, et al., Adapting the electrospinning process to provide three unique environments for a tri-layered in vitro model of the airway wall, J. Vis. Exp. 101 (2015) e52986.
[39] G.P. Duffy, T.M. McFadden, E.M. Byrne, S.L. Gill, E. Farrell, F.J. O'Brien, Towards in vitro vascularisation of collagen-GAG scaffolds, Eur. Cell Mater. 21 (2011) 15–30.
[40] K.J. Livak, T.D. Schmittgen, Analysis of relative gene expression data using real-time quantitative PCR and the 2(-Delta Delta C(T)) Method, Methods 25 (2001) 402–408.
[41] M.S. Ali, J.P. Pearson, Upper airway mucin gene expression: a review, Laryngoscope 117 (2007) 932–938.
[42] C.I. Grainger, L.L. Greenwell, D.J. Lockley, G.P. Martin, B. Forbes, Culture of Calu-3 cells at the air interface provides a representative model of the airway epithelial barrier, Pharm. Res. 23 (2006) 1482–1490.
[43] Y. You, T. Huang, E.J. Richer, J.E. Schmidt, J. Zabner, Z. Borok, et al., Role of f-box factor foxj1 in differentiation of ciliated airway epithelial cells, Am. J. Physiol. Lung Cell. Mol. Physiol. 286 (2004) L650–L657.
[44] A.I. Ivanov, C.A. Parkos, A. Nusrat, Cytoskeletal regulation of epithelial barrier function during inflammation, Am. J. Pathol. 177 (2010) 512–524.
[45] A.J. Engler, S. Sen, H.L. Sweeney, D.E. Discher, Matrix elasticity directs stem cell lineage specification, Cell 126 (2006) 677–689.
[46] C. Pohl, M.I. Hermanns, C. Uboldi, M. Bock, S. Fuchs, J. Dei-Anang, et al., Barrier functions and paracellular integrity in human cell culture models of the proximal respiratory unit, Eur. J. Pharm. Biopharm. 72 (2009) 339–349.
[47] S.C. Pageau, O.V. Sazonova, J.Y. Wong, A.M. Soto, C. Sonnenschein, The effect of stromal components on the modulation of the phenotype of human bronchial epithelial cells in 3D culture, Biomaterials 32 (2011) 7169–7180.
[48] T.M. Freyman, I.V. Yannas, R. Yokoo, L.J. Gibson, Fibroblast contraction of a collagen-GAG matrix, Biomaterials 22 (2001) 2883–2891.
[49] C.R. Lee, A.J. Grodzinsky, M. Spector, The effects of cross-linking of collagen-glycosaminoglycan scaffolds on compressive stiffness, chondrocyte-mediated contraction, proliferation and biosynthesis, Biomaterials 22 (2001) 3145–3154.
[50] D.J. Thornton, K. Rousseau, M.A. McGuckin, Structure and function of the polymeric mucins in airways mucus, Annu. Rev. Physiol. 70 (2008) 459–486.
[51] T.W. Huang, P.W. Cheng, Y.H. Chan, T.H. Yeh, Y.H. Young, T.H. Young, Regulation of ciliary differentiation of human respiratory epithelial cells by the receptor for hyaluronan-mediated motility on hyaluronan-based biomaterials, Biomaterials 31 (2010) 6701–6709.
[52] B.S. Schuster, J.S. Suk, G.F. Woodworth, J. Hanes, Nanoparticle diffusion in respiratory mucus from humans without lung disease, Biomaterials 34 (2013) 3439–3446.
[53] V. Kim, T.J. Rogers, G.J. Criner, New concepts in the pathobiology of chronic obstructive pulmonary disease, Proc. Am. Thorac. Soc. 5 (2008) 478–485.
[54] C. Blume, D.E. Davies, In vitro and ex vivo models of human asthma, Eur. J. Pharm. Biopharm. 84 (2013) 394–400.
[55] S.P. Choksi, G. Lauter, P. Swoboda, S. Roy, Switching on cilia: transcriptional networks regulating ciliogenesis, Development 141 (2014) 1427–1441.
[56] A.A. Pezzulo, T.D. Starner, T.E. Scheetz, G.L. Traver, A.E. Tilley, B.G. Harvey, et al., The air-liquid interface and use of primary cell cultures are important to recapitulate the transcriptional profile of in vivo airway epithelia, Am. J. Physiol. Lung Cell. Mol. Physiol. 300 (2011) L25–L31.
[57] B.P. Chan, K.W. Leong, Scaffolding in tissue engineering: general approaches and tissue-specific considerations, Eur. Spine J. 17 (Suppl. 4) (2008) 467–479.
[58] H. Harrington, P. Cato, F. Salazar, M. Wilkinson, A. Knox, J.W. Haycock, et al., Immunocompetent 3D model of human upper airway for disease modeling and in vitro drug evaluation, Mol. Pharm. 11 (2014) 2082–2091.
[59] B. Forbes, C. Ehrhardt, Human respiratory epithelial cell culture for drug delivery applications, Eur. J. Pharm. Biopharm. 60 (2005) 193–205.
[60] B.M. Rothen-Rutishauser, S.G. Kiama, P. Gehr, A three-dimensional cellular model of the human respiratory tract to study the interaction with particles, Am. J. Respir. Cell Mol. Biol. 32 (2005) 281–289.
[61] M.M. Choe, P.H. Sporn, M.A. Swartz, An in vitro airway wall model of remodeling, Am. J. Physiol. Lung Cell Mol. Physiol. 285 (2003) L427–L433.
[62] S. Rhee, Fibroblasts in three dimensional matrices: cell migration and matrix remodeling, Exp. Mol. Med. 41 (2009) 858–865.
[63] P.M. Crapo, T.W. Gilbert, S.F. Badylak, An overview of tissue and whole organ decellularization processes, Biomaterials 32 (2011) 3233–3243.
[64] F. Pati, J. Jang, D.H. Ha, S. Won Kim, J.W. Rhie, J.H. Shim, et al., Printing three-dimensional tissue analogues with decellularized extracellular matrix bioink, Nat. Commun. 5 (2014) 3935.
[65] L. Partington, N.J. Mordan, C. Mason, J.C. Knowles, H.W. Kim, M.W. Lowdell, et al., Biochemical changes caused by decellularization may compromise

mechanical integrity of tracheal scaffolds, Acta Biomater. 9 (2013) 5251–5261.
[66] S. Haykal, J.P. Soleas, M. Salna, S.O. Hofer, T.K. Waddell, Evaluation of the structural integrity and extracellular matrix components of tracheal allografts following cyclical decellularization techniques: comparison of three protocols, Tissue Eng. Part C Methods 18 (2012) 614–623.
[67] S. Baiguera, C. Del Gaudio, M.O. Jaus, L. Polizzi, A. Gonfiotti, C.E. Comin, et al., Long-term changes to in vitro preserved bioengineered human trachea and their implications for decellularized tissues, Biomaterials 33 (2012) 3662–3672.
[68] D. Balharry, K. Sexton, K.A. BeruBe, An in vitro approach to assess the toxicity of inhaled tobacco smoke components: nicotine, cadmium, formaldehyde and urethane, Toxicology 244 (2008) 66–76.
[69] K. BeruBe, M. Aufderheide, D. Breheny, R. Clothier, R. Combes, R. Duffin, et al., In vitro models of inhalation toxicity and disease. The report of a FRAME workshop, Altern. Lab. Anim. 37 (2009) 89–141.
[70] H.X. Ong, D. Traini, P.M. Young, Pharmaceutical applications of the Calu-3 lung epithelia cell line, Expert Opin. Drug Deliv. 10 (2013) 1287–1302.